

# Fit CATE Once: Model-Assisted Randomization Tests Without Sample Splitting

Fangnan Zheng and Yao Zhang\*

May 12, 2026

## Abstract

Randomization tests and flexible treatment-effect models offer complementary strengths for analyzing data from randomized panel experiments: the former provide valid inference under the known assignment mechanism, while the latter can capture complex patterns of effect heterogeneity. We develop model-assisted randomization tests that combine these strengths without sample splitting. The key idea is to estimate an unsigned version of the conditional average treatment effect (CATE) from the covariance structure of residualized outcomes, while leaving the realized assignments for randomization inference. The remaining sign can be chosen to best fit the observed outcomes. We establish identification and consistency for the proposed unsigned CATE estimators, as well as validity for the CATE-assisted randomization tests. Across synthetic and semi-synthetic experiments, the CATE-assisted randomization tests control Type I error and achieve higher power than covariate-adjusted and sample-split alternatives. Finally, we show that the assignment-free CATE estimates can be used to discover heterogeneous subgroups and test subgroup-specific treatment effects.

## 1 Introduction

Randomized experiments run over time produce sequences of outcomes that are well suited to studying dynamic causal effects. For example, a government rolling out an employment subsidy across regions can track annual earnings to see how the policy’s impact unfolds. Similarly, a clinical trial that staggers treatment start times

---

\*Department of Statistics and Data Science, National University of Singapore.

across patients can record symptom scores over multiple visits to learn whether effects strengthen, plateau, or fade. To recover these patterns, standard analyses often use regression models to separate treatment effects from other variation, but valid inference can become sensitive to modeling assumptions that are not always easy to justify.

This concern motivates design-based or randomization-based inference, where validity is grounded in the known assignment mechanism rather than in strong outcome-modeling assumptions. For example, randomization-based central limit theorems support asymptotically valid confidence intervals for treatment effects without an i.i.d. assumption [Li and Ding, 2017], and related ideas have been developed for time-series and panel experiments [Athey and Imbens, 2022, Bojinov and Shephard, 2019, Bojinov et al., 2021]. When baseline covariates are available, ordinary least squares adjustment with heteroskedasticity-robust standard errors yields asymptotically valid intervals even under model misspecification [Lin, 2013], and follow-up work extends this to nonlinear adjustment [Guo and Basse, 2023, Cohen and Fogarty, 2024] and to more complex designs [Lin and Ding, 2025, Gao and Ding, 2025].

In this article, we focus on randomization tests [Fisher, 1935] for causal inference. They offer finite-sample validity and allow flexible test statistics, including statistics that use regression models to detect complex treatment-effect patterns. Existing work typically adjusts the statistic with a conditional-mean model [Rosenbaum, 2002, Zhao and Ding, 2021]; a natural next step is to use a CATE model, which captures effect heterogeneity across units and time. However, naively fitting a CATE model on the realized assignments and using it in the test may break validity. One must either refit the model for every randomized assignment [Guo et al., 2025], which is usually too expensive, or use sample splitting [Zhang and Gao, 2025], which sacrifices power.

We develop an assignment-free method for estimating CATEs to construct randomization tests. Our key observation is that, under an additive outcome model, residualized outcomes can be written as centered treatment-timing indicators multiplied by lagged treatment effects, plus noise, so their second moments encode treatment-effect magnitudes. When effects are lag-invariant, diagonal residual moments identify a common effect magnitude; when residual errors are serially uncorrelated, off-diagonal moments identify the full lagged CATE vector *up to a global sign*. Because these moments depend only on covariates, outcomes, and the known assignment mechanism, they can be estimated *without* fitting on the realized assignments. The remaining sign is much simpler to learn than the full CATE surface: it can be chosen to best fit the residualized outcome trajectory, or learned from a small subset of revealed assignments. Together with the unsigned estimator, this yields a signed CATE estimator that can be used in randomization-test statistics while preserving validity.

On the theoretical side, we establish local and global identification results for our assignment-free estimation strategy and prove consistency for the proposed unsigned

CATE estimator. On the empirical side, we verify that the unsigned CATE estimator is consistent and can also warm-start signed CATE estimation when only a small number of assignments are revealed. This shows that our estimation strategy is useful not only for randomization tests, but also for direct CATE estimation. Through additional synthetic and semi-synthetic experiments, we show that our CATE-assisted randomization tests control Type I error and achieve higher power than unadjusted, covariate-adjusted, and sample-split alternatives. We also show that assignment-free CATE estimates can help reveal subgroups with heterogeneous treatment effects and construct valid randomization tests within the discovered subgroups.

The rest of the paper is organized as follows. Section 2 discusses related work. Section 3 introduces the experimental setup and the randomization-test framework. Section 4 develops the diagonal and off-diagonal residual-moment estimators for unsigned CATEs and establishes identification and consistency results. Section 5 explains how to orient the unsigned estimator and construct CATE-assisted randomization tests. Section 6 presents the experiments, and Section 7 concludes with a discussion.

## 2 Related work

Our work connects to several strands of the literature on randomized inference. The closest is the line on randomization tests with covariate adjustment. A classical starting point is Rosenbaum [2002], who studies randomization tests based on residualized outcomes from a conditional mean model. For inference on the average treatment effect, Zhao and Ding [2021] propose a robust  $t$ -statistic based on a linear model with treatment–covariate interactions. Hennessy et al. [2016] develop conditional randomization tests that restrict the assignment space to account for covariate imbalance between treated and control groups. Our work differs from this line in two ways. First, we study experiments run over time, where treatment timing creates repeated outcomes. Second, instead of using only outcome adjustment, we use residual covariances to extract treatment-effect information before randomization tests.

A second strand is the literature on design-based, or randomization-based, inference for panel and time-series experiments. Bojinov and Shephard [2019] develop causal estimands and exact randomization tests for temporal interventions in single-unit settings, while Bojinov et al. [2021] extend this design-based framework to panel experiments with repeated observations on multiple units. Most relevant to us is Zhang and Zhao [2025], who develop conditional randomization tests for lagged and spillover treatment effects without using outcome or treatment-effect models. Building on their conditioning idea, we study how to construct more powerful test statistics by estimating CATEs from residual covariances without using the realized assignments.

A third strand is the literature on staggered-adoption designs. [Athey and Imbens \[2022\]](#) analyze randomized staggered-adoption experiments from a design-based perspective. In observational settings, a large literature has shown that standard two-way fixed-effects event-study regressions can fail to recover dynamic effects under treatment-effect heterogeneity [[Goodman-Bacon, 2021](#), [Sun and Abraham, 2021](#)], prompting a range of alternative estimators [[Callaway and Sant’Anna, 2021](#), [Borusyak et al., 2024](#), [Roth et al., 2023](#)]. Our setting is different: treatment timing is randomized and known from the design, so we do not need parallel-trends assumptions. Instead, we exploit randomization directly for exact or conditional inference.

### 3 Setup

Suppose we observe a panel with  $N$  units and  $T$  time periods. For each unit  $i \in [N]$ , we observe covariates  $X_i \in \mathbb{R}^d$ , outcomes  $Y_{i,[T]} = (Y_{i,1}, \dots, Y_{i,T})$ , and a treatment start time  $A_i \in [T + 1]$ , where  $A_i = T + 1$  means a never-treated unit. For example, in a staggered-adoption design, the assignment vector  $A_{[N]}$  is drawn uniformly from all assignments with exactly  $N_t$  units starting treatment at time  $t$  for each  $t \in [T + 1]$ . We discuss other randomized panel designs in [Appendix A](#).

We impose two standard assumptions throughout. First, we assume no interference, meaning that unit  $i$ ’s outcome at time  $t$  depends only on its own treatment start time: for any  $a \in [T + 1]$ ,  $Y_{i,t} = Y_{i,t}(A_i) = Y_{i,t}(a)$  whenever  $A_i = a$ . Second, we assume no anticipation, meaning that treatment starting after time  $t$  has no effect on the time- $t$  outcome:  $Y_{i,t}(a) = Y_{i,t}(T + 1)$  for all  $a > t$ . In this article, we mainly consider testing a global sharp null and lag-specific nulls. The sharp null of no treatment effect is

$$H_0 : Y_{i,t}(a) = Y_{i,t}(T + 1) \quad \text{for all } i \in [N], 1 \leq a \leq t \leq T. \quad (1)$$

This null asks whether treatment has any effect at all. Because it is sharp, all missing potential outcomes can be imputed under  $H_0$ , making it the basic benchmark for randomization inference. In many panel experiments, however, the sharp null is too coarse: rejecting  $H_0$  does not reveal whether the effect appears immediately, emerges only after several periods, or varies with exposure length. We therefore refine the global null by introducing lag-specific null hypotheses.

Fix a time  $t \in [T - l]$  and a lag  $l \in \{0, \dots, T - 1\}$ . Define the time-specific lag- $l$  null

$$H_{0,t,l} : Y_{i,t+l}(t) = Y_{i,t+l}(T + 1) \quad \text{for all } i \in [N]. \quad (2)$$

This null asks whether treatment initiated at time  $t$  has any effect on the outcome  $l$  periods later, at time  $t + l$ . The lag- $l$  null  $H_{0,l}$  is the intersection of the time-specific nulls  $H_{0,t,l}$  over all  $t = 1, \dots, T - l$ . In other words,  $H_{0,l}$  asserts that treatment has no

effect exactly  $l$  periods after adoption, uniformly over all treatment start times. Both nulls  $H_0$  and  $H_{0,l}$  can be extended to fixed-effect null hypotheses with prespecified effect sizes, and can also be restricted to prespecified subgroups.

### 3.1 Model-assisted randomization tests

A randomization test is defined through a test statistic  $T(O_{[N]}; \hat{\eta})$ , which maps the data  $O_{[N]}$  into evidence against the null. Here  $\hat{\eta}$  denotes a nuisance model, such as regression models for the outcomes and/or treatment effects. This model is used to adjust for covariates and construct a lower-variance statistic, which can improve power by making the alternative distribution easier to distinguish from the null distribution.

Let  $\tilde{A}_{[N]}$  be an independent copy of  $A_{[N]}$  drawn from the same assignment distribution. Let  $\tilde{\mathbb{P}}$  denote the distribution of  $\tilde{A}_{[N]}$ , and let  $\tilde{O}_{[N]}$  denote the simulated dataset obtained by replacing the observed assignments in  $O_{[N]}$  with  $\tilde{A}_{[N]}$  while keeping the observed covariates and outcomes fixed. We test  $H_0$  using the  $p$ -value

$$p(O_{[N]}; \hat{\eta}) = \tilde{\mathbb{P}}_{\tilde{A}_{[N]}} \{ T(\tilde{O}_{[N]}; \hat{\eta}) \geq T(O_{[N]}; \hat{\eta}) \}. \quad (3)$$

The hypothesis  $H_{0,t,l}$  in (2) is weaker than  $H_0$ . Under  $H_{0,t,l}$  and no anticipation,

$$Y_{i,t+l}(a) = Y_{i,t+l}(a') = Y_{i,t+l}(T+1), \quad \text{for } a, a' \in \mathcal{A}_{t,l} := \{t, t+l+1, \dots, T+1\}.$$

Following Zhang and Zhao [2025], we test  $H_{0,t,l}$  using the conditional  $p$ -value

$$p_{t,l}(O_{[N]}; \hat{\eta}) = \tilde{\mathbb{P}}_{\tilde{A}_{[N]}} \{ T_{t,l}(\tilde{O}_{[N]}; \hat{\eta}) \geq T_{t,l}(O_{[N]}; \hat{\eta}) \mid g_{t,l}(\tilde{A}_{[N]}) = g_{t,l}(A_{[N]}) \}, \quad (4)$$

where  $g_{t,l}(A_{[N]}) = \{i \in [N] : A_i \in \mathcal{A}_{t,l}\}$  denotes the set of units that either start treatment at time  $t$  or remain untreated at time  $t+l$ , and the statistic  $T_{t,l}$  only depends on these units' outcomes at  $t+l$ . The conditional distribution of  $\tilde{A}_{[N]}$  in (4) can be viewed as an artificial randomized experiment among the units in  $g_{t,l}(A_{[N]})$ .

**Theorem 1.** *Assume that  $\hat{\eta} \perp\!\!\!\perp A_{[N]} \mid X_{[N]}, Y_{[N],[T]}$ . Then rejecting  $H_0$  whenever  $p(O_{[N]}; \hat{\eta}) \leq \alpha$  controls the Type I error at level  $\alpha \in (0, 1)$ :*

$$\mathbb{P}_{H_0} \{ p(O_{[N]}; \hat{\eta}) \leq \alpha \mid X_{[N]}, Y_{[N],[T]} \} \leq \alpha. \quad (5)$$

By the same randomization argument, the conditional  $p$ -value  $p_{t,l}(O_{[N]}; \hat{\eta})$  also controls the Type I error under  $H_{0,t,l}$ . The conditional independence assumption is central to (5). If it is violated, for example because  $\hat{\eta}$  is fitted using  $A_{[N]}$ , then the two test statistics in (3) are no longer equal in distribution, and the resulting  $p$ -value need not be valid. Refitting  $\hat{\eta}$  for every simulated value of  $\tilde{A}_{[N]}$  would restore this symmetry, but is often computationally prohibitive, especially when  $\hat{\eta}$  is a machine learning model.

Thus, there is a basic trade-off in constructing model-assisted randomization tests. To preserve validity, the nuisance model  $\hat{\eta}$  should not be fitted using the observed assignments  $A_{[N]}$ . But to improve power, especially for detecting treatment effects, we would like an accurate treatment-effect model. In practice, this usually leaves two choices: use only an outcome model, or estimate treatment effects by sample splitting.

We next show that repeated observations in longitudinal experiments offer a way around this trade-off. By exploiting the covariance structure of residualized outcomes, we can identify the CATE vector up to a global sign without fitting on the realized assignments. Choosing the remaining sign is much easier than estimating the full CATE from scratch, and can be guided by the observed covariates and outcomes or by a small subset of observed assignments. This leads to CATE-assisted randomization tests that preserve validity while avoiding the efficiency loss from sample splitting.

## 4 Unsigned CATE estimator

For  $t \in [T + 1]$ , we denote the probability that the treatment start time  $A_i = t$ :

$$\pi_t(x) := \mathbb{P}(A_i = t \mid X_i = x), \quad t \in [T + 1].$$

We also define the probability that treatment starts no later than time  $t$  as

$$\pi_{\leq t}(x) := \mathbb{P}(A_i \leq t \mid X_i = x) = \sum_{l=0}^{t-1} \pi_{t-l}(x).$$

All these probabilities are known from the design of an experiment.

We define the outcome function and the residuals at time  $t$  as

$$\mu_t(x) := \mathbb{E}[Y_{i,t} \mid X_i = x] \quad \text{and} \quad R_{i,t} := Y_{i,t} - \mu_t(X_i).$$

We define the expected control outcome at time  $t$  as

$$\mu_{0,t}(x) := \mathbb{E}[Y_{i,t}(T + 1) \mid X_i = x] = \mathbb{E}[Y_{i,t} \mid X_i = x, A_i > t] \quad (6)$$

by no-anticipation, which implies that  $Y_{i,t} = Y_{i,t}(T + 1)$  if unit  $i$  starts the treatment after time  $t$ . For each lag  $l \in \{0, 1, \dots, T - 1\}$  and time  $t \in [T - l]$ , we define the expected outcome at time  $t + l$ ,  $l$  steps after treatment initialization at time  $t$ , as

$$\mu_{1,t+l}(x) := \mathbb{E}[Y_{i,t+l}(t) \mid X_i = x],$$

and define the lagged CATE vector  $\tau(x) := (\tau_0(x), \dots, \tau_{T-1}(x))^\top$ , where  $\tau_l(x)$  is the lag- $l$  conditional average treatment effect (CATE), defined as

$$\tau_l(x) := \mu_{1,t+l}(x) - \mu_{0,t+l}(x). \quad (7)$$

The definition in (7) implicitly assumes that, conditional on  $X_i$ , the lag- $l$  treatment effect is invariant across treatment start times. In other words, once we condition on covariates, the expected effect  $l$  steps after adoption depends only on the exposure length  $l$ , and not on the time at which treatment begins. This assumption is reasonable when the treatment and the background environment are stable over time, but it may fail if there are time-specific factors that modify treatment effects, such as seasonality, aggregate shocks, or changes in treatment implementation.

Without using the treatment assignments  $A_{[N]}$ , we can estimate the *second-order moments* of the residual vector  $R_i = (R_{i,1}, \dots, R_{i,T})^\top$ , defined by

$$\Sigma_R(x) := \mathbb{E}[R_i R_i^\top \mid X_i = x], \quad c_{t,s}(x) := [\Sigma_R(x)]_{t,s} = \mathbb{E}[R_{i,t} R_{i,s} \mid X_i = x]. \quad (8)$$

Under the model introduced below, estimating the CATE vector  $\tau(X_i)$  using the treatment assignments  $A_{[N]}$  is straightforward and admits a closed-form expression; we will discuss this estimation strategy in Section B.

## 4.1 Additive outcome model

**Assumption 1.** We posit the additive model for observed outcomes over time:

$$Y_{i,t} = \mu_{0,t}(X_i) + \sum_{l=0}^{t-1} \mathbf{1}_{\{A_i=t-l\}} \tau_l(X_i) + \epsilon_{i,t}, \quad t \in [T], \quad (9)$$

where  $\epsilon_{i,t}$  satisfies  $\mathbb{E}[\epsilon_{i,t} \mid X_i, A_i] = 0, t \in [T]$ .

Assumption 1 is flexible in several respects. The untreated mean  $\mu_{0,t}(x)$  is allowed to vary arbitrarily with both covariates and calendar time, and the treatment effect  $\tau_l(x)$  may be heterogeneous in  $x$  and depend on the exposure length  $l$ . Thus, the model does not impose linearity or parametric structure on either the baseline outcome or the dynamic treatment effect. Its key restriction is an additive mean structure: conditional on  $X_i$  and  $A_i$ , treatment shifts the outcome mean by a lag-specific amount, while the remaining error has mean zero. This formulation is reasonable when treatment primarily affects the conditional mean, and when the dynamic treatment response is stable across treatment start times after conditioning on covariates. It may fail, however, if the effect at a given lag varies across cohorts or calendar time, or if treatment interacts with unobserved variables in a non-additive way. Additional restrictions on the second moments of  $\epsilon_i$  are imposed below only where needed.

In (9), the sum has at most one nonzero term because  $A_i$  takes a single value: if  $A_i = t - l$  then the sum is the lag- $l$  effect  $\tau_l(X_i)$ , while if  $A_i > t$  (not yet treated) then

the entire sum is zero. Following the transform of [Robinson \[1988\]](#), we residualize (9) by subtracting off its expectation given  $X_i$ , which yields

$$R_{i,t} = Y_{i,t} - \mu_t(X_i) = \sum_{l=0}^{t-1} \left( \mathbf{1}_{\{A_i=t-l\}} - \pi_{t-l}(X_i) \right) \tau_l(X_i) + \epsilon_{i,t}. \quad (10)$$

Equation (10) rewrites the residual  $R_{i,t}$  as the sum of a treatment component and a noise component. The treatment component is a linear combination of the centered indicators  $\mathbf{1}_{\{A_i=t-l\}} - \pi_{t-l}(X_i)$ , which have mean zero conditional on  $X_i$ . Moreover, since  $A_i$  takes a single value, the treatment component measures how  $A_i$  deviates from its expectation, scaled by the lagged effect  $\tau_l(X_i)$ . Rewrite (10) in matrix form

$$R_i = \Pi(X_i) \tau(X_i) + \epsilon_i,$$

where  $\epsilon_i := (\epsilon_{i,1}, \dots, \epsilon_{i,T})^\top$  and  $\Pi(X_i)$  is a  $T \times T$  random assignment matrix with

$$[\Pi(X_i)]_{t,l+1} = [\mathbf{1}_{\{A_i=t-l\}} - \pi_{t-l}(X_i)] \mathbf{1}_{\{l \leq t-1\}}, \quad \forall t \in [T], \quad l = 0, 1, \dots, T-1.$$

Substituting  $R_i$  into the second moments  $\Sigma_R(x)$  in (8), we obtain a decomposition

$$\begin{aligned} \Sigma_R(x) &= \Sigma_A(x; \tau) + \Sigma_\epsilon(x), \\ \Sigma_A(x; \tau) &:= \mathbb{E}[\Pi(X_i) \tau(X_i) \tau(X_i)^\top \Pi(X_i)^\top \mid X_i = x], \\ \Sigma_\epsilon(x) &:= \mathbb{E}[\epsilon_i \epsilon_i^\top \mid X_i = x]. \end{aligned} \quad (11)$$

This decomposition provides a unified set of conditional moment restrictions. Because  $\Sigma_A(x; \tau)$  depends on  $\tau(x)$  only through  $\tau(x) \tau(x)^\top$ , all second-order restrictions are invariant to a *global* sign flip  $\tau(x) \mapsto -\tau(x)$ . Thus,  $\tau(x)$  is identified up to an overall sign unless an additional normalization is imposed (e.g., the lag-0 effect  $\tau_0(x) \geq 0$ ). Different structural assumptions lead to different estimating equations for  $\tau(x)$ .

## 4.2 Estimation from diagonal moments

We begin with a simplified setting in which the treatment effect is constant across lags. Under this assumption, the diagonal entries of  $\Sigma_R(x)$  take a particularly simple form and already suffice to identify the treatment-effect magnitude.

**Assumption 2.** For any  $x \in \mathcal{X}$  and any  $l \in \{0, \dots, T-1\}$ , the lag- $l$  effect is constant:

$$\tau_l(x) \equiv \tau_*(x).$$

**Assumption 3** (Time-invariant residual variance). For any  $x \in \mathcal{X}$ ,

$$\mathbb{E}[\epsilon_{i,t}^2 \mid X_i = x] = \sigma_\epsilon^2(x), \quad t \in [T].$$

Assumption 2 reduces the lagged CATE vector to a single effect  $\tau_*(x)$ , while Assumption 3 makes the residual noise contribution common across time. Together, they imply that changes in the diagonal residual moments across  $t$  are driven by the known design factor  $v_t(x)$ , which allows us to identify  $\tau_*^2(x)$ . If residual variances vary over time, these diagonal moments would confound treatment-effect magnitude with time-varying noise.

**Proposition 1.** *Suppose Assumptions 1, 2, and 3 hold. Then, for each  $t \in [T]$ ,*

$$c_{t,t}(x) = [\Sigma_R(x)]_{t,t} = \tau_*^2(x) v_t(x) + \sigma_\epsilon^2(x), \quad v_t(x) := \pi_{\leq t}(x)(1 - \pi_{\leq t}(x)).$$

Under the additive model in Assumption 1, the time- $t$  outcome depends on whether treatment has started by time  $t$ . The diagonal term  $c_{t,t}(x) = \mathbb{E}[R_{i,t}^2 \mid X_i = x]$  is the conditional variance of the residualized outcome at time  $t$ . Proposition 1 shows that under the lag-invariant effect assumption, this variance has two components: variation from randomized treatment timing, equal to  $\tau_*^2(x)v_t(x)$ , and residual outcome noise, equal to  $\sigma_\epsilon^2(x)$ . The coefficient  $v_t(x)$  is known from the design. Thus, the only unknowns in the identity are the squared treatment-effect magnitude  $\tau_*^2(x)$  and the nuisance variance  $\sigma_\epsilon^2(x)$ . Because  $\sigma_\epsilon^2(x)$  is common across  $t$ , we can eliminate it by comparing diagonal moments over time. Averaging the identity in Proposition 1 gives

$$\bar{c}(x) := \frac{1}{T} \sum_{t=1}^T c_{t,t}(x) = \tau_*^2(x) \bar{v}(x) + \sigma_\epsilon^2(x), \quad \bar{v}(x) := \frac{1}{T} \sum_{t=1}^T v_t(x).$$

**Proposition 2.** *Suppose Assumptions 1, 2, and 3 hold. Fix  $x \in \mathcal{X}$ . If there exists  $t \in [T]$  such that  $v_t(x) \neq \bar{v}(x)$ , the magnitude  $m_*(x) := |\tau_*(x)|$  is point identified, with*

$$m_*(x) = \sqrt{\frac{c_{t,t}(x) - \bar{c}(x)}{v_t(x) - \bar{v}(x)}}}.$$

Proposition 2 shows that, after removing the common nuisance term  $\sigma_\epsilon^2(x)$  by differencing across time, the remaining variation in the diagonal moments identifies  $\tau_*^2(x)$ . The key requirement is that the design generate nontrivial variation in  $v_t(x)$  across  $t$ ; otherwise, the diagonal moments do not contain enough information to separate  $\tau_*^2(x)$  from  $\sigma_\epsilon^2(x)$ . Since the moment equation identifies only the squared effect,  $\tau_*(x)$  is identified up to sign. Motivated by Proposition 2, we let

$$\hat{\tau}_\pm^{\text{diag}}(x) := \hat{m}_*(x) I_T, \quad I_T = (1, \dots, 1)^\top \in \mathbb{R}^T, \quad (12)$$

where we estimate  $m_*(x)$  by plugging in estimators of the diagonal moments:

$$\hat{m}_*(x) := \sqrt{\max \left\{ \frac{\hat{c}_{t,t}(x) - \hat{\bar{c}}(x)}{v_t(x) - \bar{v}(x)}, 0 \right\}}, \quad \hat{\bar{c}}(x) := \frac{1}{T} \sum_{t=1}^T \hat{c}_{t,t}(x).$$

**Proposition 3.** *Suppose Assumptions 1, 2, and 3 hold. Fix  $x \in \mathcal{X}$ , and suppose there exists  $t \in [T]$  such that  $v_t(x) \neq \bar{v}(x)$ . If  $\hat{c}_{t,t}(x) \xrightarrow{p} c_{t,t}(x)$  for all  $t \in [T]$ , then*

$$\hat{m}_*(x) \xrightarrow{p} m_*(x).$$

Proposition 3 shows that the plug-in magnitude estimator  $\hat{m}_*(x)$  is consistent for  $m_*(x) = |\tau_*(x)|$ . If it is known a priori that  $\tau_*(x) \geq 0$ , we can recover the treatment effect itself by  $\hat{\tau}_*(x) = \hat{m}_*(x)$ , which satisfies  $\hat{\tau}_*(x) \xrightarrow{p} \tau_*(x)$ . Note that (12) yields one estimator for each  $t \in [T]$  with  $v_t(x) \neq \bar{v}(x)$ . These estimators may differ in finite samples, so we aggregate them to obtain the final estimator of  $m_*(x)$ .

### 4.3 Estimation from off-diagonal moments

We next consider the more general case in which the CATEs may vary across lags. In this setting, off-diagonal moments become informative because, under the next assumption, residual errors are uncorrelated over time. Thus, any off-diagonal residual covariance comes from treatment timing and lag-specific treatment effects.

**Assumption 4.** For any  $x \in \mathcal{X}$ ,  $\Sigma_\epsilon(x)$  is diagonal, i.e.,

$$\mathbb{E}[\epsilon_{i,t}\epsilon_{i,s} \mid X_i = x] = 0 \quad \text{for all } t \neq s.$$

This assumption is reasonable when the remaining outcome shocks are approximately uncorrelated over time after accounting for covariates. It may fail in settings with latent shocks or other sources of serial dependence. Let  $\mathcal{P} := \{(t, s) : 1 \leq s < t \leq T\}$ , and collect the off-diagonal moments from (8) into the vector

$$c(x) := (c_{t,s}(x))_{(t,s) \in \mathcal{P}} \in \mathbb{R}^{T(T-1)/2}.$$

**Proposition 4.** *Under Assumptions 1 and 4,  $c(x)$  has the quadratic representation*

$$c(x) = F_x(\tau) := (\tau^\top H_{t,s}(x)\tau)_{(t,s) \in \mathcal{P}}, \quad (13)$$

where each  $H_{t,s}(x) \in \mathbb{R}^{T \times T}$  is a symmetric matrix depending only on the treatment assignment probabilities  $\pi_a(x)$ ,  $a \in [T + 1]$ .

Proposition 4 shows that the off-diagonal residual covariances depend on the CATE vector  $\tau(x)$  through quadratic forms. They therefore contain information about all components of  $\tau(x)$ , not just the common magnitude identified by the diagonal moments. Since Assumption 4 removes the off-diagonal error covariance, any remaining covariance between residuals at different time points must come from the shared treatment-timing indicators and the lag-specific treatment effects. This turns estimation of the lagged CATE vector into a moment-matching problem.

### 4.3.1 Estimators

To approximate the identity (13), we estimate  $c(x)$  by  $\hat{c}(x)$ , obtained by regressing the estimated residual products  $\hat{R}_{i,t}\hat{R}_{i,s}$  on  $X_i$  for all  $(t, s) \in \mathcal{P}$ , and then solve

$$\hat{\tau}_{\pm}^{\text{nls}}(x) \in \arg \min_{\tau} \ell^{\text{nls}}(\tau; \hat{c}, x, \rho), \quad (14)$$

where  $\ell^{\text{nls}}(\tau; \hat{c}, x, \rho)$  is the *pointwise* nonlinear least-squares (NLS) objective

$$\ell^{\text{nls}}(\tau; \hat{c}, x, \rho) := \|\hat{c}(x) - F_x(\tau)\|_2^2 + \rho \|\tau\|_2^2,$$

and  $\rho \geq 0$  is a ridge penalty. Because  $F_x(\tau)$  takes the same value at  $\tau(x)$  and  $-\tau(x)$ , the true  $\tau(x)$  is identifiable only up to sign. This is the same basic ambiguity that arises in other quadratic inverse problems [Shechtman et al., 2015, Candès et al., 2013, 2015]. Below, we show that this is the only ambiguity under a local rank condition.

The objective function in (14) is nonconvex, so standard optimization methods such as Gauss–Newton or Levenberg–Marquardt may converge only to local minima. Our consistency result therefore applies to a global minimizer of the NLS objective; in computation, we use the convex relaxation below to provide a stable initialization and reduce the risk of converging to a poor local minimum.

Define  $\mathcal{A}_x(B) := (\text{tr}(H_{t,s}(x)B))_{(t,s) \in \mathcal{P}}$ . When  $B = \tau\tau^\top$ , this gives the trace-form representation of the right-hand side of (13). We estimate  $B(x) = \tau(x)\tau(x)^\top$  by

$$\hat{B}(x) \in \arg \min_{B \succeq 0} \ell^{\text{cvx}}(B; \hat{c}, x, \lambda), \quad (15)$$

where  $\ell^{\text{cvx}}(B; \hat{c}, x, \lambda)$  is the convex objective

$$\ell^{\text{cvx}}(B; \hat{c}, x, \lambda) := \|\hat{c}(x) - \mathcal{A}_x(B)\|_2^2 + \lambda \text{tr}(B).$$

On the positive semidefinite cone, the trace penalty encourages a low-rank solution, reflecting the rank-one structure of  $B(x)$ . We solve (15) using a standard semidefinite programming solver. Since  $T$  is small in our applications, the matrix variable  $B \in \mathbb{R}^{T \times T}$  has only  $T(T+1)/2$  free entries, so this step is computationally modest. After obtaining  $\hat{B}(x)$ , we compute its top eigenpair  $(\hat{\lambda}_1(x), \hat{u}_1(x))$  and define the spectral estimator

$$\hat{\tau}_{\pm}^{\text{sp}}(x) := \sqrt{\hat{\lambda}_1(x)} \hat{u}_1(x). \quad (16)$$

The two estimators play different roles. The NLS criterion targets the CATE vector  $\tau(x)$  directly, but is nonconvex. The convex relaxation instead targets the rank-one matrix  $B(x) = \tau(x)\tau(x)^\top$ , which can be estimated more stably and whose leading eigenvector provides a natural initializer for local optimization of the NLS objective. The result below also shows that, even without the NLS refinement step, the spectral estimator obtained from the convex relaxation can be itself consistent up to sign.

### 4.3.2 Identification & Consistency

Define the compact parameter spaces

$$\Theta := \{\tau \in \mathbb{R}^T : \|\tau\|_2 \leq M\}, \quad \mathbb{B} := \{B \succeq 0 : \text{tr}(B) \leq M^2\}.$$

Let  $J_x(\tau) := \frac{\partial F_x(\tau)}{\partial \tau^\top} \in \mathbb{R}^{|\mathcal{P}| \times T}$  denote the Jacobian of the moment map.

**Proposition 5** (Local identification up to sign). *Fix  $x \in \mathcal{X}$ . Suppose  $\tau(x) \neq 0$  and  $\text{rank}(J_x(\tau(x))) = T$ . Then there exists an open neighborhood  $\mathcal{N}_x$  of  $\tau(x)$  such that*

$$\{\tau \in \mathcal{N}_x \cup (-\mathcal{N}_x) : F_x(\tau) = c(x)\} = \{\tau(x), -\tau(x)\}.$$

*Locally,  $B(x) = \tau(x)\tau(x)^\top$  is point identified, while  $\tau(x)$  is identified up to sign.*

Proposition 5 exploits the quadratic structure of  $F_x(\tau) := (\tau^\top H_{t,s}(x)\tau)_{(t,s) \in \mathcal{P}}$ . It shows that, in a neighborhood of the true CATE vector, the quadratic moment equations identify the full vector  $\tau(x)$  up to the unavoidable global sign. This is useful because the map  $F_x(\tau)$  is nonlinear and symmetric in  $\tau$ , so a priori the off-diagonal moments could fail to distinguish many nearby CATE vectors.

The rank condition rules this out locally. For a small perturbation  $h \in \mathbb{R}^T$ , the corresponding change in the  $(t, s)$ -th moment is

$$(\tau(x) + h)^\top H_{t,s}(x)(\tau(x) + h) - \tau(x)^\top H_{t,s}(x)\tau(x) = 2h^\top H_{t,s}(x)\tau(x) + h^\top H_{t,s}(x)h.$$

Thus, to first order, the effect of perturbing  $\tau(x)$  is determined by the vectors

$$\{H_{t,s}(x)\tau(x) : (t, s) \in \mathcal{P}\}.$$

The rank condition  $\text{rank}(J_x(\tau(x))) = T$  is equivalent to

$$\text{span}\{H_{t,s}(x)\tau(x) : (t, s) \in \mathcal{P}\} = \mathbb{R}^T.$$

There are  $|\mathcal{P}| = \binom{T}{2}$  such vectors in  $\mathbb{R}^T$ , so for  $T \geq 3$ , the off-diagonal moments provide at least as many restrictions as there are lag-specific effects. This makes the full-rank condition reasonable in standard treatment assignment designs. However, it is not automatic: the vectors may still be linearly dependent or nearly redundant if the assignment probabilities provide little variation across treatment times, or if the true effect vector  $\tau(x)$  lies in an unfavorable direction.

To make the full-rank condition more concrete, the next proposition gives a simple example where the rank can be checked under equal assignment probability  $q$ . In this example, checking full rank boils down to a much simpler scalar check: whether a polynomial  $P_{T,\rho}(q)$  is nonzero for the given  $T$ ,  $\rho$ , and  $q$ . Equal assignment probabilities and decaying CATE patterns are common in practice, but this example is not meant to cover every design satisfying the full-rank condition.

**Proposition 6** (A sufficient equal-probability design). *Fix  $T \geq 3$  and  $x \in \mathcal{X}$ . Suppose the treatment start time is assigned independently of  $X_i$ , with*

$$\pi_1(x) = \cdots = \pi_T(x) = q, \quad \pi_{T+1}(x) = 1 - Tq,$$

*for some  $q \in (0, 1/T)$ . Suppose the lagged CATE follows a geometric decay pattern*

$$\tau_l(x) = \theta(x)\rho^l, \quad l = 0, \dots, T-1,$$

*where  $\theta(x) \neq 0$  and  $\rho \in (0, 1)$ . Then there exists a nonzero polynomial  $P_{T,\rho}(q)$  such that, whenever  $P_{T,\rho}(q) \neq 0$ , we have  $\text{rank}(J_x(\tau(x))) = T$ .*

The condition  $P_{T,\rho}(q) \neq 0$  should be interpreted as a generic nondegeneracy condition on the assignment probabilities. In the proof,  $P_{T,\rho}(q)$  arises as the determinant of a  $T \times T$  submatrix of the Jacobian, after factoring out the nonzero scale  $\theta(x)^T$ . The key point is that this determinant is a nonzero polynomial in  $q$ . Hence it can vanish only at finitely many values of  $q$ . Therefore, for fixed  $T$  and  $\rho$ , the full-rank condition holds for all equal-probability designs except for a finite set of exceptional assignment probabilities. Equivalently, if  $q$  were chosen from any continuous distribution on  $(0, 1/T)$ , the rank condition would hold with probability one. In applications, one need not compute the polynomial explicitly; the rank of  $J_x(\hat{\tau}(x))$ , or the conditioning of the corresponding Jacobian, can be checked numerically for the chosen design.

The local identification result in Proposition 5 provides the basis for the global condition: it shows that no nearby CATE vector can reproduce the same moments, apart from the global sign flip. The global condition then only needs to rule out distant spurious solutions. Intuitively, when the treatment assignment design is sufficiently informative, these quadratic equations should determine  $\tau(x)$  uniquely up to this unavoidable sign ambiguity. To formalize this, define the sign-invariant distance

$$d_{\pm}(u, v) := \min\{\|u - v\|_2, \|u + v\|_2\}. \quad (17)$$

**Proposition 7** (Global identification up to sign). *Fix  $x \in \mathcal{X}$ . Suppose  $\tau(x) \in \Theta$ , and suppose that for every  $\varepsilon > 0$ ,*

$$\inf_{\tau \in \Theta: d_{\pm}(\tau, \tau(x)) \geq \varepsilon} \|F_x(\tau) - c(x)\|_2^2 > 0.$$

*Then  $\tau(x)$  is globally identified up to a single global sign on  $\Theta$ , in the sense that*

$$\{\tau \in \Theta : F_x(\tau) = c(x)\} = \{\tau(x), -\tau(x)\}.$$

*Consequently,  $B(x) = \tau(x)\tau(x)^\top$  is globally point identified on  $\Theta$ .*

Proposition 7 strengthens the local identification result in Proposition 5 from a neighborhood of  $\tau(x)$  to the full parameter space  $\Theta$ . It rules out distant CATE vectors that reproduce the same off-diagonal residual covariances as  $\tau(x)$ , except for the unavoidable global sign flip. This is the condition that prevents a global minimizer of the NLS objective from converging to a distant spurious solution.

For the convex relaxation, we use the analogous matrix-level condition stated in Theorem 2:  $B(x) = \tau(x)\tau(x)^\top$  is the unique minimizer of the population convex objective over  $\mathbb{B}$ . This condition rules out alternative positive semidefinite matrices  $B \neq \tau(x)\tau(x)^\top$  that produce the same off-diagonal moments. Once  $B(x) = \tau(x)\tau(x)^\top$  is uniquely identified, its leading eigenvector recovers the direction of  $\tau(x)$ , up to a global sign. Thus the spectral estimator targets the equivalence class  $\{\tau(x), -\tau(x)\}$ .

**Assumption 5.** Suppose  $N \rightarrow \infty$ ,

- (i) for any  $x \in \mathcal{X}$ ,  $\hat{c}(x) \xrightarrow{P} c(x)$ ;
- (ii) for any compact  $\mathcal{X}_0 \subset \mathcal{X}$ ,  $\sup_{x \in \mathcal{X}_0} \|\hat{c}(x) - c(x)\|_2 \xrightarrow{P} 0$ .

**Assumption 6** (Regularity and boundedness). Fix a compact  $\mathcal{X}_0 \subset \mathcal{X}$ . Assume:

- (i)  $H_{t,s}(x)$  is continuous in  $x$  for all  $(t, s) \in \mathcal{P}$ ;
- (ii)  $\sup_{x \in \mathcal{X}_0} \max_{(t,s) \in \mathcal{P}} \|H_{t,s}(x)\|_{\text{op}} < \infty$ ;
- (iii)  $\sup_{x \in \mathcal{X}_0} \|\tau(x)\|_2 \leq M < \infty$ .

**Theorem 2** (Consistency of convex relaxation). *Suppose Assumptions 5–6 hold. Fix  $x \in \mathcal{X}_0$ . Assume that  $B(x) := \tau(x)\tau(x)^\top$  is the unique minimizer of  $\ell^{\text{cvx}}(B; c, x, 0)$  over  $\mathbb{B}$ . Then any minimizer  $\hat{B}(x)$  of  $\ell^{\text{cvx}}(B; \hat{c}, x, \lambda)$  over  $\mathbb{B}$ , with  $\lambda = o(1)$ , satisfies*

$$\|\hat{B}(x) - B(x)\|_F \xrightarrow{P} 0, \quad \text{as } N \rightarrow \infty.$$

Moreover, if  $\|\tau(x)\|_2 \geq c_\tau$  for some  $c_\tau > 0$ , then the spectral estimator  $\hat{\tau}_\pm^{\text{sp}}(x)$  satisfies

$$d_\pm(\hat{\tau}_\pm^{\text{sp}}(x), \tau(x)) \xrightarrow{P} 0, \quad \text{as } N \rightarrow \infty.$$

Theorem 2 has two implications. First, the convex program consistently recovers the rank-one matrix  $B(x)$ . Second, once  $B(x)$  is recovered, the leading eigenvector consistently recovers  $\tau(x)$  up to a global sign. This justifies the program as a stable route to recovering the signal structure before resolving the remaining sign ambiguity.

**Theorem 3** (Consistency of NLS). *Suppose Assumptions 5–6 hold. Fix  $x \in \mathcal{X}_0$ . Assume that  $\ell^{\text{nls}}(\tau; c, x, 0)$  has the unique minimizer set  $\{\tau(x), -\tau(x)\}$  over  $\Theta$ . Then any global minimizer  $\hat{\tau}_\pm^{\text{nls}}(x)$  of  $\ell^{\text{nls}}(\tau; \hat{c}, x, \rho)$  over  $\Theta$ , with  $\rho = o(1)$ , satisfies*

$$d_\pm(\hat{\tau}_\pm^{\text{nls}}(x), \tau(x)) \xrightarrow{P} 0.$$

Theorem 3 shows that any global NLS minimizer consistently recovers the lagged CATE vector up to a global sign. Relative to the convex relaxation, the NLS criterion targets  $\tau(x)$  directly rather than the intermediate matrix  $B(x)$ . The price is computational rather than statistical: the theorem applies to global minimizers, whereas numerical algorithms may find only local stationary points. This is why, in practice, the convex estimator is useful as a warm start even when the final target is the NLS solution.

## 5 CATE-assisted randomization tests

Given an unsigned CATE estimator from the previous section, we now explain how to orient it and use it to construct a CATE-assisted randomization test.

### 5.1 Orienting the unsigned CATE estimator

Let  $\hat{\tau}_{\pm}(x) = (\hat{\tau}_{\pm,0}(x), \dots, \hat{\tau}_{\pm,T-1}(x))^{\top}$  denote an unsigned CATE estimator. This may be the diagonal estimator  $\hat{\tau}_{\pm}^{\text{diag}}(x)$  from Section 4.2, or the off-diagonal spectral or NLS estimators  $\hat{\tau}_{\pm}^{\text{sp}}(x)$  and  $\hat{\tau}_{\pm}^{\text{nls}}(x)$  from Section 4.3. If the sign of  $\tau_l(x)$  is known for some lag  $l$ , we can choose between  $\hat{\tau}_{\pm}(x)$  and  $-\hat{\tau}_{\pm}(x)$  to match that sign.

When no prior sign information is available, we choose the sign that best fits the residualized outcome trajectory in (10). Specifically, for each unit  $i$ , define

$$\hat{s}_i = \arg \min_{s \in \{-1, 1\}} \left\{ \min_{a \in [T+1]} \sum_{t=1}^T \left[ \hat{R}_{i,t} - \sum_{l=0}^{t-1} \left( \mathbf{1}_{\{a=t-l\}} - \pi_{t-l}(X_i) \right) s \hat{\tau}_{\pm,l}(X_i) \right]^2 \right\}. \quad (18)$$

This criterion chooses the sign that makes the residualized outcome path most compatible with the estimated treatment effects, allowing the treatment start time  $a$  to vary over its possible values. Equivalently, the squared loss can be viewed as a Gaussian working negative log-likelihood for the residualized outcomes conditional on  $X_i$  and a candidate treatment start time. We then define the signed CATE estimator by

$$\hat{\tau}(X_i) := \hat{s}_i \hat{\tau}_{\pm}(X_i).$$

Because  $\hat{s}_i$  is chosen using unit  $i$ 's residual trajectory,  $\hat{\tau}(X_i)$  should be understood as a fixed unit-level signed CATE estimate at the observed covariate value  $X_i$ , rather than as a newly fitted function on all of  $\mathcal{X}$ . The test statistics below only require these fitted values for the observed units  $i \in [N]$ .

We orient the CATE vector separately for each unit. This step is not guaranteed to recover the correct sign for every unit, even if the other nuisance estimators are

consistent. The reason is simple: each unit provides only one finite outcome trajectory, and we do not use its realized treatment start time  $A_i$  when choosing the sign. Although  $A_i$  is randomized, the covariates and outcomes still contain information about which treatment start time best explains the residual trajectory. Unless this prediction of  $A_i$  is perfect, the selected sign can be wrong. The next proposition makes this precise in an oracle setting, where the unsigned CATE is known or well estimated.

**Proposition 8** (Oracle sign recovery with observed assignment). *Suppose that*

(i) *the assignment design is balanced,  $\pi_t(x) = 1/(T + 1)$  for  $t \in [T + 1]$ ;*

(ii) *the lagged CATE vector  $\tau(X_i)$  satisfies, for  $l = 0, \dots, T - 1$ ,*

$$\tau_l(X_i) = s_i \theta(X_i) \rho^l, \quad s_i \in \{-1, 1\}, \quad \theta(X_i) > 0, \quad \rho \in (0, 1);$$

(iii) *Assumption 1 holds, and conditional on  $X_i$  and  $A_i$ , the error vector  $\epsilon_i$  is mean-zero sub-Gaussian with variance proxy  $\sigma^2$ .*

Let  $\hat{s}_i^{\text{obs}}$  be the oracle sign estimator obtained from the loss in (18), using the true residuals and the true CATE magnitudes  $|\tau_l(X_i)| = \theta(X_i) \rho^l$ , with the observed assignment  $A_i$  fixed in the loss. Then, for any unit with  $A_i = a \leq T$ ,

$$\mathbb{P}(\hat{s}_i^{\text{obs}} \neq s_i \mid X_i, A_i = a) \leq \exp \left\{ -\frac{\theta^2(X_i)}{2\sigma^2} \left( 1 - \frac{a}{T + 1} \right)^2 \right\}.$$

Proposition 8 is an oracle benchmark for the sign-learning problem. It fixes the realized assignment  $A_i$ , so the remaining task is only to choose between two signs. In this simplified setting, where first-stage estimation error is ignored, the probability of choosing the wrong sign is governed by a simple signal-to-noise ratio and the treatment start time. The bound is not meant to be sharp; it uses a simple lower bound to make the intuition transparent. First, the bound shows that the sign is easier to recover when the effect scale  $\theta(X_i)$  is large and the noise variance  $\sigma^2$  is small. Second, the bound shows why early treatment starts are especially helpful for sign recovery. If  $A_i = a$  is small, then many later outcomes are post-treatment, so the signed treatment effect appears repeatedly across the outcome path. If  $a$  is close to  $T$ , most outcomes are pre-treatment and only a few observations carry information about the signed effect. In that case, the two signs are much harder to tell apart.

The fully assignment-free rule in (18) is more delicate because it does not observe  $A_i$ . Suppose, for the moment, that we ignore first-stage estimation error. Under the

correct sign  $s_i$ , the loss for a candidate time  $\tilde{a}$  is

$$\begin{aligned}\ell_i^+(\tilde{a}) &= \sum_{t=1}^T \left[ R_{i,t} - \sum_{l=0}^{t-1} \left( \mathbf{1}_{\{\tilde{a}=t-l\}} - \pi_{t-l}(X_i) \right) s_i \theta(X_i) \rho^l \right]^2 \\ &= \sum_{t=1}^T \left[ \epsilon_{i,t} + s_i \theta(X_i) \left\{ \mathbf{1}_{\{A_i \leq t\}} \rho^{t-A_i} - \mathbf{1}_{\{\tilde{a} \leq t\}} \rho^{t-\tilde{a}} \right\} \right]^2.\end{aligned}$$

Thus, in the noiseless case,  $\ell_i^+(\tilde{a})$  is minimized at  $\tilde{a} = A_i$ . A misspecified start time, especially one far from  $A_i$ , creates a systematic mismatch along the residual trajectory. With noise, however, exact recovery of  $A_i$  is not necessary for sign recovery. Define

$$\ell_i(s) = \min_{\tilde{a} \in [T+1]} \sum_{t=1}^T \left[ R_{i,t} - \sum_{l=0}^{t-1} \left( \mathbf{1}_{\{\tilde{a}=t-l\}} - \pi_{t-l}(X_i) \right) s \theta(X_i) \rho^l \right]^2.$$

The sign is recovered whenever  $\ell_i(s_i) < \ell_i(-s_i)$ : the best-fitting trajectory under the correct sign only needs to beat the best-fitting trajectory under the wrong sign.

A complementary strategy is to use a small subset of observed assignments only for sign learning. This orients  $\hat{\tau}_{\pm}$  while keeping most units available for randomization inference. Importantly, this is still much simpler than estimating the full CATE from the labeled subset, because the second stage only needs to choose the sign. We revisit this point in the experiments, where a small fraction of observed assignments is enough to orient  $\hat{\tau}_{\pm}$  effectively and produce an accurate signed CATE estimator.

## 5.2 CATE-assisted test statistics

Let  $\hat{\eta}$  collect the nuisance functions used to construct the test statistic:

$$\hat{\eta} = (\hat{\mu}_1, \dots, \hat{\mu}_T, \hat{\tau}_0, \dots, \hat{\tau}_{T-1}, \pi_1, \dots, \pi_{T+1}).$$

The nuisance quantities in  $\hat{\eta}$  are constructed from the observed covariates, outcomes, and the known assignment mechanism, without fitting on the realized assignments. Hence they satisfy the conditional independence condition required in Theorem 1.

Once we obtain the unit-level signed CATE estimates  $\hat{\tau}(X_i)$ , we use the additive outcome model in Assumption 1 to estimate the control outcome functions by

$$\hat{\mu}_{0,t}(X_i) := \hat{\mu}_t(X_i) - \sum_{s=0}^{t-1} \pi_{t-s}(X_i) \hat{\tau}_s(X_i), \quad t \in [T],$$

and the lag- $l$  treated outcome functions by

$$\hat{\mu}_{1,t+l}(X_i) := \hat{\mu}_{0,t+l}(X_i) + \hat{\tau}_l(X_i), \quad l \in \{0, \dots, T-t\}.$$

---

**Algorithm 1:** CATE-assisted randomization test
 

---

1. For each  $t \in [T]$ , fit  $\hat{\mu}_t(\cdot)$  by regressing  $Y_{i,t}$  on  $X_i$ , and compute the residuals

$$\hat{R}_{i,t} := Y_{i,t} - \hat{\mu}_t(X_i), \quad i \in [N].$$

2. Estimate the residual covariance matrix  $\Sigma_R(x)$  in (8) by regressing  $\hat{R}_{i,t}\hat{R}_{i,s}$  on  $X_i$ :

$$\hat{c}_{t,s}(x) = \widehat{\mathbb{E}}[\hat{R}_{i,t}\hat{R}_{i,s} \mid X_i = x], \quad t, s \in [T].$$

3. Estimate the CATE vector up to a global sign:
  - (a) If the effect is lag-invariant, use the diagonal estimator  $\hat{\tau}_{\pm}^{\text{diag}}(x)$  in (12).
  - (b) If the effect varies across lags, use the off-diagonal spectral estimator  $\hat{\tau}_{\pm}^{\text{SP}}(x)$  from (16), and optionally refine it to  $\hat{\tau}_{\pm}^{\text{nls}}(x)$  using (14).

4. Orient the unsigned estimator using (18), and set  $\hat{\tau}(X_i) = \hat{s}_i \hat{\tau}_{\pm}(X_i)$ ,  $i \in [N]$ .

5. Compute a CATE-assisted randomization statistic and its  $p$ -value using the signed estimator  $\hat{\tau}$ , the outcome estimators  $\hat{\mu}_t$ , and the known probabilities  $\pi_a(x)$ .
- 

To test the time-specific lag- $l$  hypothesis  $H_{0,t,l}$  in (2), we use a statistic of the form

$$T_{t,l}(O_{[N]}; \hat{\eta}) = \frac{1}{N} \sum_{i=1}^N \psi_{i,t,l}(O_i; \hat{\eta}), \quad (19)$$

where  $\psi_{i,t,l}(O_i; \hat{\eta})$  is a unit-level score designed to detect the lag- $l$  effect.

For example, one can use the augmented inverse probability weighting (AIPW) score [Robins et al., 1994] for the average lag- $l$  treatment effect at time  $t$ :

$$\psi_{i,t,l}^{\text{AIPW}}(O_i; \hat{\eta}) := \hat{\tau}_l(X_i) + \frac{\mathbf{1}_{\{A_i=t\}}}{\pi_t(X_i)} \left\{ Y_{i,t+l} - \hat{\mu}_{1,t+l}(X_i) \right\} - \frac{\mathbf{1}_{\{A_i>t+l\}}}{1 - \pi_{\leq t+l}(X_i)} \left\{ Y_{i,t+l} - \hat{\mu}_{0,t+l}(X_i) \right\}.$$

Here, units with  $A_i = t$  form the treated group at lag  $l$ , while units with  $A_i > t + l$  remain untreated at time  $t + l$  and serve as controls.

Alternatively, suppose we want a test statistic that is more directly sensitive to heterogeneous treatment effects across units. Motivated by a Gaussian working model with common variance, we can use the following likelihood-ratio score for the alternative  $\tau_l(X_i) = \hat{\tau}_l(X_i)$  against the null  $\tau_l(X_i) = 0$ :

$$\begin{aligned} \psi_{i,t,l}^{\text{LR}}(O_i; \hat{\eta}) &= -[Y_{i,t+l} - \hat{\mu}_{0,t+l}(X_i) - \mathbf{1}_{\{A_i=t\}}\hat{\tau}_l(X_i)]^2 + [Y_{i,t+l} - \hat{\mu}_{0,t+l}(X_i)]^2 \\ &= \mathbf{1}_{\{A_i=t\}} \left\{ 2\hat{\tau}_l(X_i)[Y_{i,t+l} - \hat{\mu}_{0,t+l}(X_i)] - \hat{\tau}_l^2(X_i) \right\}. \end{aligned} \quad (20)$$

The Gaussian model is used only to motivate the score  $\psi_{i,t,l}^{\text{LR}}(O_i; \hat{\eta})$ ; validity of the randomization test still follows from the random assignment mechanism.

To test the sharp null  $H_0$  in (1), we aggregate the lag-specific statistics as

$$T(O_{[N]}; \hat{\eta}) = \frac{1}{T} \sum_{l=0}^{T-1} \frac{1}{T-l} \sum_{t=1}^{T-l} T_{t,l}(O_{[N]}; \hat{\eta}).$$

Algorithm 1 summarizes the construction of the CATE-assisted randomization test. Depending on the identifying assumptions, we use either diagonal or off-diagonal residual moments to estimate the CATE vector up to sign, orient the unsigned estimator, and use the signed CATE estimator and other outcome function estimators to define a test statistic. As described in Section 3.1, we use this statistic to compute a randomization  $p$ -value  $p(O_{[N]}; \hat{\eta})$  for the hypothesis of interest.

## 6 Experiments

This section evaluates the finite-sample performance of our CATE-assisted randomization tests, checks convergence of the unsigned CATE estimators, and presents semi-synthetic experiments based on county teen employment data. Code to reproduce the experiments is available at <https://github.com/fangnanzheng/fit-cate-once>.

### 6.1 Synthetic data

We compare four randomization tests (RTs), using either no covariate adjustment or different forms of covariate adjustment. All tests use the statistic form in (19), but differ in the choice of the test score  $\psi_{i,t,l}(O_i; \hat{\eta})$ . The regression models used in the statistics are fitted using gradient boosting regression trees.

- **RT (DM)** uses the difference between the treated and not-yet-treated means:

$$\psi_{i,t,l}^{\text{DM}}(O_i) = \frac{N}{N_t} \mathbf{1}_{\{A_i=t\}} Y_{i,t+l} - \frac{N}{N_{>t+l}} \mathbf{1}_{\{A_i>t+l\}} Y_{i,t+l},$$

where  $N_{>t+l} = \sum_{s=t+l+1}^{T+1} N_s$  is the number of not-yet-treated units at time  $t+l$ .

- **RT (cDM)** uses the same mean-difference statistic after residualizing outcomes:

$$\psi_{i,t,l}^{\text{cDM}}(O_i; \hat{\eta}) = \frac{N}{N_t} \mathbf{1}_{\{A_i=t\}} [Y_{i,t+l} - \hat{\mu}_{t+l}(X_i)] - \frac{N}{N_{>t+l}} \mathbf{1}_{\{A_i>t+l\}} [Y_{i,t+l} - \hat{\mu}_{t+l}(X_i)].$$

- **RT (SS)** uses the likelihood-ratio score  $\psi_{i,t,l}^{\text{LR}}(O_i; \hat{\eta})$  in (20), where the CATE estimator is constructed using the realized assignments of 50% of the units, following the method in Section B. This method is based on Assumption 1 and is the closest comparison to our assignment-free CATE estimation method. The remaining 50% of the units are used for the randomization test.
- **RT (CATE)** is our proposed randomization test, implemented as in Algorithm 1, and also uses the likelihood-ratio score  $\psi_{i,t,l}^{\text{LR}}(O_i; \hat{\eta})$ .

We consider a randomized staggered-adoption experiment with  $T = 5$  time periods and sample size  $N \in \{300, 400, 500, 600, 700\}$ . For each unit  $i \in [N]$ , we observe covariates  $X_i = (X_{i,1}, \dots, X_{i,5})$ . The first four covariates are drawn independently from  $\text{Unif}[-2, 2]$ . The fifth covariate  $X_{i,5} \mid X_{i,1} \sim \text{Bernoulli}(0.08/[1 + \exp(-X_{i,1})])$ . Each unit receives a treatment start time  $A_i \in \{1, 2, 3, 4, 5, 6\}$ , where  $A_i = 6$  denotes never treated. The cohort proportions are  $\pi = (0.1, 0.2, 0.2, 0.2, 0.2, 0.1)$ . For each  $N$ , the cohort counts are obtained by rounding  $N\pi$ . Conditional on these cohort counts, units are randomly assigned to the six treatment-timing groups. This can be viewed as a completely randomized experiment over treatment start times.

For the Type I error control experiments, we set  $\tau_l(X_i) = 0$  for all units  $i$  and all lags  $l$ , while keeping the parts of the data distribution unchanged. For the power experiments, we use the treatment-effect functions specified below.

### 6.1.1 Lag-invariant treatment effects

Under Assumption 2, we implement our method using the diagonal estimator from Section 4.2. To match the lag-invariant treatment-effect assumption, we generate outcomes  $Y_{i,t}$  as in (9), with  $\Sigma_\epsilon(X_i) = (2^{-|t-s|})_{t,s=1}^T$ . For  $t \in [5]$  and  $l = 0, \dots, 4$ , set

$$\mu_{0,t}(X_i) = (0.7 + 0.1t) \sum_{j=1}^5 X_{i,j}, \quad \tau_l(X_i) = 3.5X_{i,5} - 0.1(1 - X_{i,5}).$$

Since the CATE is lag-invariant, we test the global null. In addition, we partition the covariate space into  $K = 5$  subgroups  $\mathcal{S}_k := \{i \in [N] : X_i \in \mathcal{X}_k\}$ ,  $k \in [K]$ , where  $\mathcal{X}_k$ 's are created evenly using the four quintile cut-points of  $X_{i,1}$ . We test the subgroup null

$$H_{0,k} : Y_{i,t}(a) = Y_{i,t}(T+1) \quad \text{for all } i \in \mathcal{S}_k, 1 \leq a \leq t \leq T. \quad (21)$$

This subgroup null asks whether treatment has no effect within each subgroup  $k$ . Testing these subgroup nulls is useful when treatment effects may be heterogeneous across covariates, while testing the global null could miss important structure.

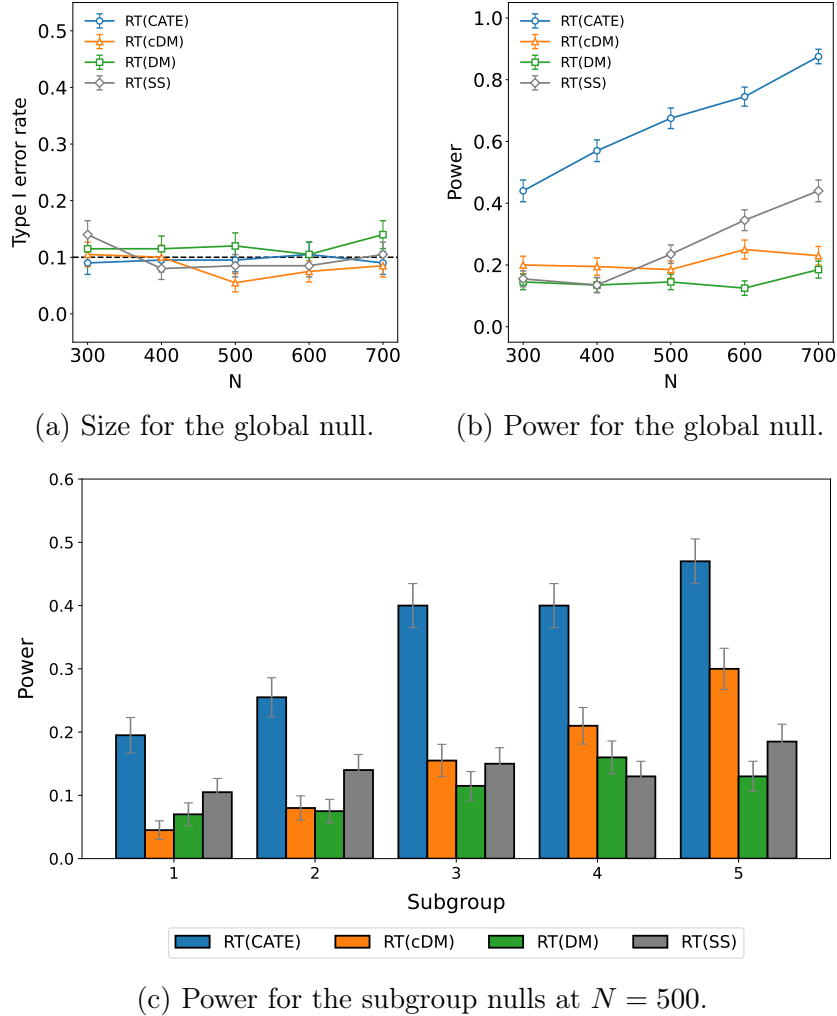


Figure 1: Comparison of randomization tests under the lag-invariant effect assumption.

Figure 1 reports the size and power results for all randomization tests. The  $p$ -values are computed using 500 randomization draws, and rejection rates are evaluated at the nominal level  $\alpha = 0.1$ . All results are averaged over 200 experimental replications.

Figure 1a confirms that all four randomization tests control Type I error near the nominal level 0.1. Building upon this validity check, Figure 1b shows that RT (CATE) achieves the highest power across all sample sizes. RT (CATE) outperforms RT (cDM) because it uses the CATE estimator to detect not only average treatment effects but also heterogeneous treatment effects across units.

Figure 1c shows that RT (CATE) also achieves the highest power for the subgroup nulls in (21). In the data-generating process, treatment effects become stronger from subgroup 1 to 5. Accordingly, the power of RT (CATE) and RT (cDM) increases across subgroups, while the power of RT (DM) and RT (SS) remains relatively stable.

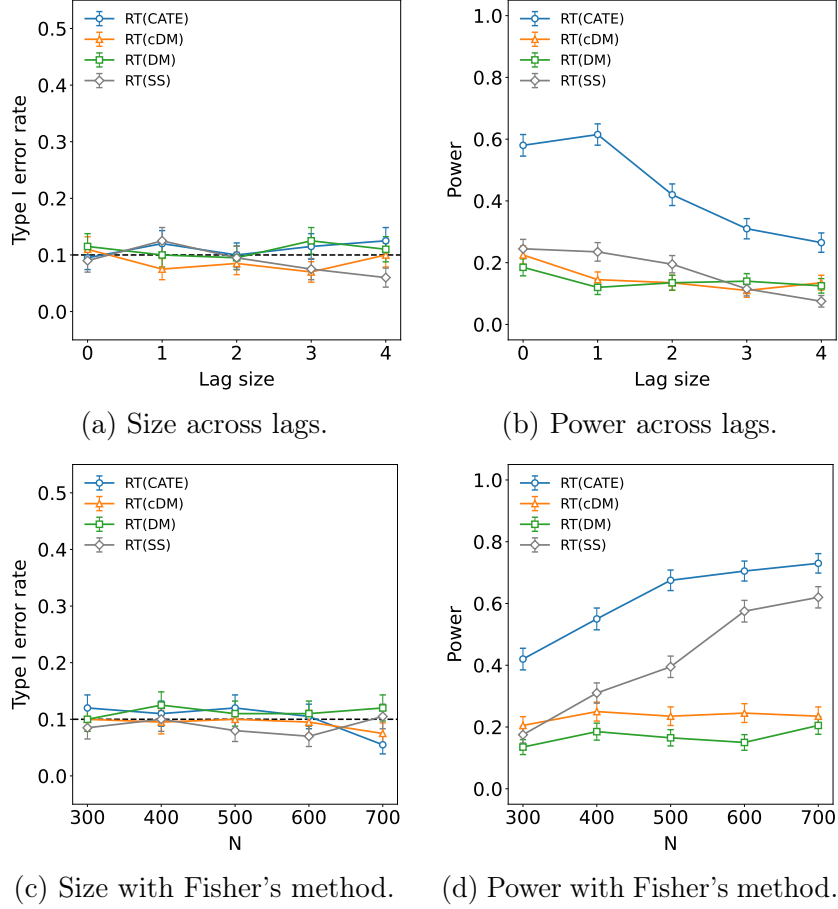


Figure 2: Comparison of randomization tests under the lagged-effect assumption. The top row tests lagged effects at time  $t = 1$ . The bottom row reports the results obtained by using Fisher's method combining  $p$ -values across time  $t$  for  $l = 0$ .

### 6.1.2 Lagged treatment effects

Under Assumption 4, we implement our method using the off-diagonal estimator from Section 4.3. We generate outcomes  $Y_{i,t}$  with lag-varying treatment effects:

$$\mu_{0,t}(X_i) = (0.7 + 0.1t) \sum_{j=1}^5 X_{i,j}, \quad \tau_l(X_i) = 0.9^l (3.5X_{i,5} - 0.1(1 - X_{i,5})),$$

for  $t \in [5]$  and  $l = 0, \dots, 4$ , with error covariance  $\Sigma_\epsilon(X_i) = I_T$ .

We first test the lag- $l$  effect at adoption time  $t = 1$  for  $l = 0, \dots, 4$ . We also test the global lag-0 null by combining  $p$ -values from the time-specific lag-0 tests across all time steps, using the conditional randomization test in Zhang and Zhao [2025].

Figure 2 reports the size and power results for all tests. The  $p$ -values are computed using 500 randomization draws, and rejection rates are evaluated at the nominal level  $\alpha = 0.1$ . All results are averaged over 200 experimental replications. Figures 2a and 2c confirm that all randomization tests control size near the nominal level, both for the individual lag-specific nulls and for the global lag-0 null. Figures 2b and 2d show that RT (CATE) achieves higher power than the other methods for detecting lagged effects, both before and after combining the  $p$ -values with Fisher’s method.

## 6.2 Consistency and warm-starting experiments

We next provide a modest empirical check of the identification and consistency theory in Section 4.3.2. We ask two practical questions: whether the assignment-free unsigned CATE estimator can converge to the true CATE up to a global sign, and whether it can serve as a useful warm start for learning the signed CATE vector.

We focus on the off-diagonal unsigned CATE estimator in Section 4.3. In Algorithm 1, we use gradient-boosted regression trees to estimate the outcome functions and the residual covariance matrix. We first compute the spectral estimator in (16), and then refine it by solving the NLS problem in (14). We set the trace penalty in the convex relaxation to decrease with the sample size, while always using no ridge penalty in the NLS refinement. Other details of this experiment, including the data-generating process, are given in Appendix C.1. We also repeat the consistency experiment with a finite-dimensional parametric version of the off-diagonal estimator in Appendix C.2.

Let  $\hat{\tau}_{\pm, N}$  denote the unsigned estimator at sample size  $N$ . Figure 3a shows that the normalized mean squared error (NMSE) of  $\hat{\tau}_{\pm, N}$  decreases toward zero as  $N$  increases. The NMSE is defined using the unsigned distance  $d_{\pm}(\cdot, \cdot)$  in (17):

$$\text{NMSE}(\hat{\tau}_{\pm, N}, \tau) = \frac{\mathbb{E}[d_{\pm}\{\hat{\tau}_{\pm, N}(X), \tau(X)\}^2]}{\mathbb{E}[\|\tau(X)\|_2^2]}.$$

For the warm-start experiment, we fix a full dataset of size  $N = 25,600$ . We first fit the off-diagonal estimator using all covariates and outcomes. We then reveal assignments for  $M \in \{25, 50, 100, 200, 400, 800, 1600, 3200\}$  units. We compare two estimators: a direct R-learner [Nie and Wager, 2020] that learns the full CATE vector from these  $M$  assignment-revealed units, and a warm-start estimator that learns only the missing sign on top of our unsigned CATE estimator. Both estimators are implemented using the same gradient-boosted regression trees. The warm-start estimator uses the same second-stage loss as the direct R-learner, but restricts the fitted CATE to be a signed version of the unsigned estimator; see Appendix C.1 for details.

Figure 3b reports the NMSE of the direct R-learner and our warm-start estimator, denoted by Ours, computed using the usual  $\ell_2$  distance. When  $M$  is small, the

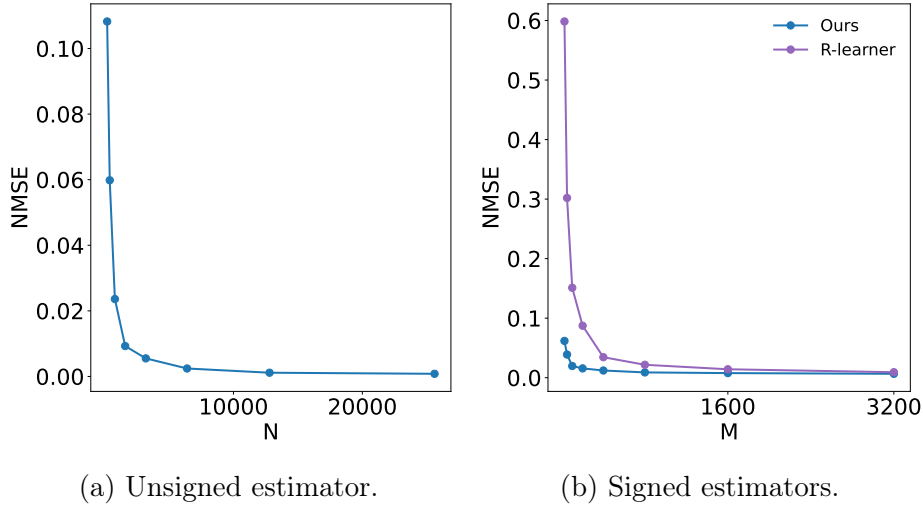


Figure 3: Normalized MSE (NMSE) of the unsigned and signed CATE estimators.

warm-start estimator is substantially more accurate. This shows that the unsigned CATE estimator can greatly reduce the number of revealed assignments needed to learn a signed CATE vector. As  $M$  grows, the direct learner improves and catches up.

The main takeaway is that learning the sign of the CATE is much easier than learning the entire CATE vector from scratch. Thus, if predicting the sign from covariates and outcomes alone is a concern, one can instead learn it from a small subset of assignments, preserving most assignments for the randomization test.

### 6.3 Experiments on county teen employment data

We next compare our randomization-test-based method with event-study two-way fixed-effects (TWFE) regression in a semi-synthetic experiment based on the minimum-wage and teen-employment dataset analyzed by Callaway and Sant’Anna [2021].<sup>1</sup> This empirical setting is a canonical staggered-adoption difference-in-differences application: counties become treated when their state raises its minimum wage, and the outcome is county-level log teen employment. In the original application, Callaway and Sant’Anna [2021] find negative average effects of minimum-wage increases on teen employment, with evidence varying across treatment cohorts. The dataset contains a balanced five-period county panel with staggered treatment adoption. We retain the county-level log-population covariate, re-randomize treatment timing using fixed cohort shares, and regenerate outcomes using the semi-synthetic model described in Appendix C.3.

We use event-study TWFE as the benchmark because it is a common specification

<sup>1</sup>The dataset is available at <https://bcallaway11.github.io/did/reference/mpdta.html>.

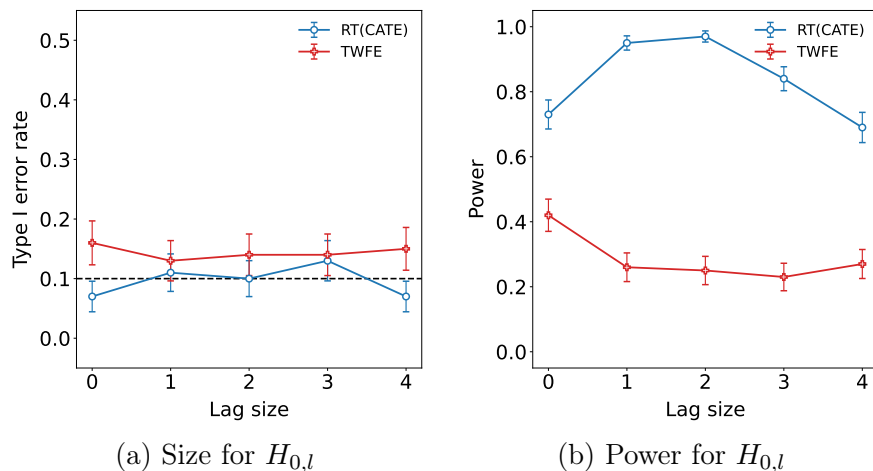


Figure 4: Semi-synthetic testing results on the county teen employment panel.

for staggered-adoption panels when treatment effects may vary with exposure length. At the same time, recent work has shown that TWFE coefficients can be difficult to interpret under treatment-effect heterogeneity. In such settings, event-study TWFE coefficients need not correspond to clean lag-specific causal effects; instead, they may combine information from different cohorts, calendar periods, and event times through regression-implied weights. Thus, event-study TWFE is a useful and familiar benchmark, but it is not designed to target the heterogeneous CATE structure exploited by the likelihood ratio statistics in our randomization test; see [Goodman-Bacon \[2021\]](#), [Sun and Abraham \[2021\]](#), [Callaway and Sant’Anna \[2021\]](#).

### 6.3.1 Comparison with TWFE model

Because the treatment effect may vary with exposure length, we use the following event-study TWFE regression:

$$Y_{i,t} = \alpha_i + \lambda_t + \sum_{l=0}^3 \beta_l \mathbf{1}_{\{A_i=t-l\}} + \beta_{\geq 4} \mathbf{1}_{\{A_i \leq t-4\}} + \sum_{h=2}^4 \delta_{-h} \mathbf{1}_{\{A_i=t+h\}} + \varepsilon_{i,t}.$$

Here  $\alpha_i$  absorbs time-invariant county differences, and  $\lambda_t$  absorbs period-specific shocks common to all counties. The coefficients  $\beta_l$ ,  $l = 0, \dots, 3$ , correspond to post-treatment event times, while  $\beta_{\geq 4}$  pools observations at least four periods after adoption into a single long-run event-time bin. We omit the period immediately before adoption as the reference period. The lead coefficients  $\delta_{-h}$ ,  $h = 2, \dots, 4$ , capture differences relative to this omitted pre-treatment period. In empirical applications, nonzero lead coefficients are often interpreted as evidence of pre-treatment imbalance or anticipation. In our semi-synthetic design, the null DGP assumes no anticipation, so these coefficients are best viewed as finite-sample diagnostics rather than structural anticipation effects.

Figures 4a and 4b report the lag-specific testing results. Under the null, event-study TWFE mildly over-rejects, with rejection rates between 13% and 16% across lags. RT (CATE) remains close to the nominal level. Under the alternative, event-study TWFE achieves rejection rates between 23% and 42%. RT (CATE) is more powerful, with rejection rates between 69% and 97% across lags. Thus, both methods show some sensitivity to the alternative, but the CATE-assisted randomization statistic produces a much sharper separation between the null and alternative. The power pattern of RT (CATE) mainly reflects the simulated lag-specific effects together with the number of available timing comparisons, which are most favorable at intermediate lags.

## 6.4 Post-randomization subgroup analysis

We now turn to a more qualitative use of the same assignment-free CATE estimates. Instead of using them only to build a more powerful test statistic, we ask whether they can also reveal useful subgroup structure after randomization.

We denote county log population by  $X_i = \text{lpop}_i$ . We generate treatment effects using a threshold model: counties above the empirical 0.65-quantile of  $X_i$  form the effective subgroup, while counties at or below the threshold form a true null subgroup. Specifically, if  $c^*$  denotes this threshold, then  $\tau_l(X_i) = -\tau_* \mathbf{1}_{\{X_i > c^*\}}$ ,  $l = 0, \dots, 4$ , where  $\tau_* \in \{0.10, 0.15, 0.20, 0.25, 0.30\}$ . Thus, the high-lpop group has a negative lag-invariant treatment effect, while the low-lpop group has no treatment effect.

We estimate the signed CATE using the diagonal residual-moment estimator and regression trees. After obtaining the fitted signed CATE values  $\hat{\tau}_i$ , we estimate the threshold by fitting a regression stump in  $X_i$ . For each candidate threshold  $c$ , we split counties into  $\{i : X_i \leq c\}$  and  $\{i : X_i > c\}$ , and choose the split that best fits the estimated CATE values. We use bootstrap bagging to compute a lower quantile  $\hat{c}$  of the selected thresholds to avoid overestimating the true threshold. The estimated low-effect group is  $\{i : X_i \leq \hat{c}\}$ , and the estimated high-effect group is  $\{i : X_i > \hat{c}\}$ . Full details of the subgroup data-generating process, threshold selection, and subgroup randomization statistic are given in Appendix C.3.2.

Figure 5 visualizes the estimated CATE functions for multiple signal levels. Our method locates the true threshold accurately and recovers the main subgroup structure. Figure 6a shows that the threshold estimate becomes more concentrated around the true threshold as the signal level  $\tau_*$  increases. Figure 6b shows that, in the estimated low-effect group where the true effect is mostly zero, the rejection rate for testing the subgroup null stays close to the nominal level. Figure 6c shows that, in the estimated high-effect group where the true treatment effect is negative, the rejection rate is close to one. These results show that the assignment-free CATE estimates can recover useful subgroup structure and support subgroup-specific randomization inference.

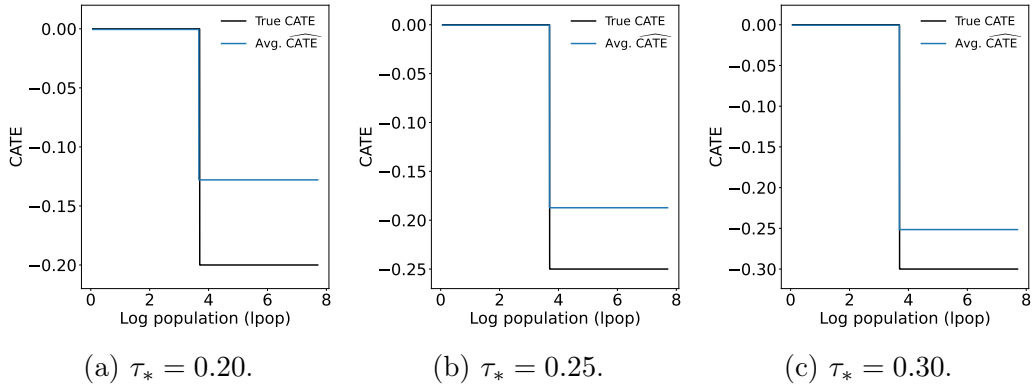


Figure 5: Estimated CATEs and thresholds for three signal levels,  $\tau_* = 0.20, 0.25, 0.30$ .

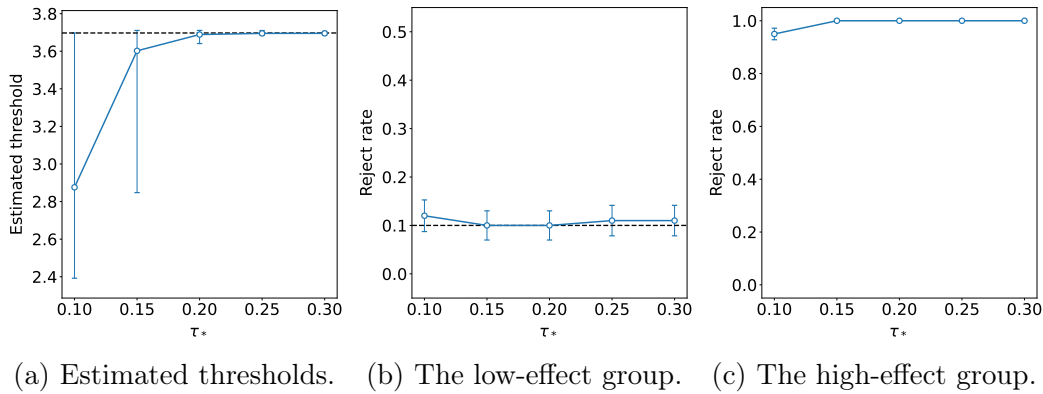


Figure 6: Estimated thresholds and rejection rates for  $\tau_* \in \{0.10, 0.15, \dots, 0.30\}$ .

## 7 Discussion

We developed a method for constructing CATE-assisted randomization tests without sample splitting. The main idea is simple: in panel experiments, residualized outcomes contain more information than their conditional means alone. Under suitable structure, their covariance matrix carries information about treatment-effect structure, and this information can be extracted without fitting on the realized assignment.

This perspective is not limited to the panel setting studied here. Similar structure may arise whenever each unit contributes multiple outcomes, or when multiple units can be matched on covariates so that their conditional outcome distributions are similar. More broadly, our results suggest a class of model-assisted randomization tests based on assignment-free treatment effect estimation. The basic ingredients are a known treatment assignment mechanism, residuals that depend on the assignment only through the treatment effects, and enough second-order moment restrictions to

identify the effect pattern of interest. The remaining sign ambiguity can often be resolved, and is a smaller problem than estimating the full CATE surface.

Several extensions seem worth pursuing. One is to extend the idea to more complex designs. Our theory imposes no strong assumptions on the panel design, so the same residual-covariance idea may still apply. The challenge is that the moment equations may become more complicated as the design becomes richer. A second direction is to relax the uncorrelated-error assumption used by the off-diagonal estimator. In many panel applications, residual errors are correlated over time. Then the off-diagonal residual covariances contain both treatment-effect information and error correlation, and separating the two is difficult. A third direction is to move beyond second-order moments: higher-order residual moments may contain sign information directly, which could give a better handle on the sign ambiguity.

## References

- Susan Athey and Guido W. Imbens. Design-based analysis in difference-in-differences settings with staggered adoption. *Journal of Econometrics*, 226(1):62–79, 2022.
- Iavor Bojinov and Neil Shephard. Time series experiments and causal estimands: exact randomization tests and trading. *Journal of the American Statistical Association*, 114(528):1665–1682, 2019.
- Iavor Bojinov, Ashesh Rambachan, and Neil Shephard. Panel experiments and dynamic causal effects: A finite population perspective. *Quantitative Economics*, 12(4):1171–1196, 2021.
- Kirill Borusyak, Xavier Jaravel, and Jann Spiess. Revisiting event-study designs: robust and efficient estimation. *The Review of Economic Studies*, 91(6):3253–3285, 2024. doi: 10.1093/restud/rdae007.
- Brantly Callaway and Pedro H. C. Sant’Anna. Difference-in-Differences with multiple time periods. *Journal of Econometrics*, 225(2):200–230, 2021. doi: 10.1016/j.jeconom.2020.12.001.
- Brantly Callaway and Pedro H.C. Sant’Anna. Difference-in-differences with multiple time periods. *Journal of Econometrics*, 225(2):200–230, 2021.
- Emmanuel J. Candès, Thomas Strohmer, and Vladislav Voroninski. Phaselift: Exact and stable signal recovery from magnitude measurements via convex programming. *Communications on Pure and Applied Mathematics*, 66(8):1241–1274, 2013.

- Emmanuel J. Candès, Xiaodong Li, and Mahdi Soltanolkotabi. Phase retrieval via wirtinger flow: Theory and algorithms. *IEEE Transactions on Information Theory*, 61(4):1985–2007, 2015.
- Peter L Cohen and Colin B Fogarty. No-harm calibration for generalized oaxaca–blinder estimators. *Biometrika*, 111(1):331–338, 2024.
- Ronald Aylmer Fisher. *Design of experiments*. Oliver and Boyd, Edinburgh, 1935.
- Mengsi Gao and Peng Ding. Causal inference in network experiments: regression-based analysis and design-based properties. *Journal of Econometrics*, 252:106119, 2025.
- Andrew Goodman-Bacon. Difference-in-differences with variation in treatment timing. *Journal of Econometrics*, 225(2):254–277, 2021. doi: 10.1016/j.jeconom.2021.03.014.
- Kevin Guo and Guillaume Basse. The generalized oaxaca-blinder estimator. *Journal of the American Statistical Association*, 118(541):524–536, 2023.
- Wenxuan Guo, JungHo Lee, and Panos Toulis. ML-assisted randomization tests for detecting treatment effects in a/b experiments. *arXiv preprint arXiv:2501.07722*, 2025.
- Jonathan Hennessy, Tirthankar Dasgupta, Luke Miratrix, Cassandra Pattanayak, and Pradipta Sarkar. A conditional randomization test to account for covariate imbalance in randomized experiments. *Journal of Causal Inference*, 4(1):61–80, 2016. doi: 10.1515/jci-2015-0018.
- Xinran Li and Peng Ding. General forms of finite population central limit theorems with applications to causal inference. *Journal of the American Statistical Association*, 112(520):1759–1769, 2017.
- Winston Lin. Agnostic notes on regression adjustments to experimental data: Re-examining freedman’s critique. *The Annals of Applied Statistics*, pages 295–318, 2013.
- Zhexiao Lin and Peng Ding. Unifying regression-based and design-based causal inference in time-series experiments. *arXiv preprint arXiv:2510.22864*, 2025.
- X Nie and S Wager. Quasi-oracle estimation of heterogeneous treatment effects. *Biometrika*, 108(2):299–319, 2020.
- James M. Robins, Andrea Rotnitzky, and Lue P. Zhao. Estimation of regression coefficients when some regressors are not always observed. *Journal of the American Statistical Association*, 89(427):846–866, 1994.
- Peter M. Robinson. Root-N-consistent semiparametric regression. *Econometrica*, 56(4):931–954, 1988. doi: 10.2307/1912705.

- Paul R. Rosenbaum. Covariance adjustment in randomized experiments and observational studies. *Statistical Science*, 17(3):286–327, 2002. doi: 10.1214/ss/1042727942.
- Jonathan Roth, Pedro H. C. Sant’Anna, Alyssa Bilinski, and John Poe. What’s trending in Difference-in-Differences? a synthesis of the recent econometrics literature. *Journal of Econometrics*, 235(2):2218–2244, 2023. doi: 10.1016/j.jeconom.2023.03.008.
- Yoav Shechtman, Yonina C. Eldar, Oren Cohen, Henry N. Chapman, Jianwei Miao, and Mordechai Segev. Phase retrieval with application to optical imaging: A contemporary overview. *IEEE Signal Processing Magazine*, 32(3):87–109, 2015.
- Liyang Sun and Sarah Abraham. Estimating dynamic treatment effects in event studies with heterogeneous treatment effects. *Journal of econometrics*, 225(2):175–199, 2021.
- Yao Zhang and Zijun Gao. Adaptive sample splitting for randomization tests, 2025. URL <https://arxiv.org/abs/2504.21572>.
- Yao Zhang and Qingyuan Zhao. Multiple conditional randomization tests for lagged and spillover treatment effects. *Biometrika*, 112(1):3–16, 2025. doi: 10.1093/biomet/asae042.
- Anqi Zhao and Peng Ding. Covariate-adjusted Fisher randomization tests for the average treatment effect. *Journal of Econometrics*, 225(2):278–294, 2021. doi: 10.1016/j.jeconom.2021.04.007.

## A Randomized panel designs

**Example 1** (Staggered-adoption design). Fix group sizes  $N_1, \dots, N_{T+1}$  such that  $\sum_{t=1}^{T+1} N_t = N$ . Here  $N_t$  denotes the number of units assigned to begin treatment at time  $t \in [T]$ , and  $N_{T+1}$  denotes the number of never-treated units. The assignment vector  $A_{[N]}$  is drawn uniformly from all assignments with these fixed group sizes:

$$\mathbb{P}(A_{[N]} = a_{[N]}) = \frac{\prod_{t=1}^{T+1} N_t!}{N!} \mathbb{1} \left\{ a_{[N]} \in [T+1]^N, \sum_{i=1}^N \mathbf{1}_{\{a_i=t\}} = N_t \text{ for all } t \in [T+1] \right\}.$$

Equivalently, exactly  $N_t$  units are assigned  $A_i = t$  for each  $t \in [T+1]$ , with  $A_i = T+1$  corresponding to never treated.

**Example 2** (Single-time adoption design). Fix a treatment time  $t^* \in [T]$ . Exactly  $N_t$  units are randomly assigned to begin treatment at time  $t^*$ , while the remaining  $N_c = N - N_t$  units are never treated. Equivalently,  $A_i \in \{t^*, T+1\}$  for all  $i$ , with exactly  $N_t$  units assigned  $A_i = t^*$ . The assignment vector  $A_{[N]}$  follows

$$\mathbb{P}(A_{[N]} = a_{[N]}) = \binom{N}{N_t}^{-1} \mathbb{1} \left\{ a_{[N]} \in \{t^*, T+1\}^N, \sum_{i=1}^N \mathbf{1}_{\{a_i=t^*\}} = N_t \right\}.$$

**Example 3** (Two-period crossover design). Fix a washout time  $t_0 \in \{1, \dots, T-1\}$ , which partitions the study into two periods: period 1 ( $t \leq t_0$ ) and period 2 ( $t > t_0$ ). Units are assigned switching times  $S_i = (A_i^{\text{on}}, A_i^{\text{off}}) \in [T+1]^2$ . Exactly  $N_{\text{AB}}$  units are assigned  $S_i = (1, t_0 + 1)$ , corresponding to treatment in period 1 and no treatment in period 2, while the remaining units are assigned  $S_i = (t_0 + 1, T+1)$ , corresponding to no treatment in period 1 and treatment in period 2. The assignment distribution is

$$\mathbb{P}(S_{[N]} = s_{[N]}) = \binom{N}{N_{\text{AB}}}^{-1} \mathbb{1} \{s_{[N]} \in \mathcal{S}_{\text{CO}}\},$$

where  $\mathcal{S}_{\text{CO}}$  denotes the set of all assignments with  $N_{\text{AB}}$  units assigned  $S_i = (1, t_0 + 1)$ .

## B Estimating equations when $A_i$ is observed

If the realized start time  $A_i$  is observed, then (10) implies linear moment equations for estimating  $\{\tau_l(\cdot)\}$ . For  $k \in \{0, 1, \dots, t-1\}$ , define

$$d_{t,k}(x) := \mathbb{E} \left[ R_{i,t} \left( \mathbf{1}_{\{A_i=t-k\}} - \pi_{t-k}(X_i) \right) \middle| X_i = x \right]. \quad (22)$$

Multiplying (10) by  $\mathbf{1}_{\{A_i=t-k\}} - \pi_{t-k}(X_i)$  and taking conditional expectations gives

$$d_{t,k}(x) = \sum_{l=0}^{t-1} \mathbb{E}[(\mathbf{1}_{\{A_i=t-l\}} - \pi_{t-l}(X_i))(\mathbf{1}_{\{A_i=t-k\}} - \pi_{t-k}(X_i)) | X_i = x] \tau_l(x),$$

where the noise term drops by  $\mathbb{E}[\epsilon_{i,t} | X_i, A_i] = 0$ . Using mutual exclusivity of the indicators  $\{\mathbf{1}_{\{A_i=a\}} : a \in [T+1]\}$ , this simplifies to

$$d_{t,k}(x) = \pi_{t-k}(x)\tau_k(x) - \pi_{t-k}(x) \sum_{l=0}^{t-1} \pi_{t-l}(x)\tau_l(x). \quad (23)$$

Assume that  $1 - \pi_{\leq t}(x) > 0$ . Summing (23) over  $k = 0, \dots, t-1$  and rearranging yields

$$\sum_{l=0}^{t-1} \pi_{t-l}(x)\tau_l(x) = \frac{\sum_{k=0}^{t-1} d_{t,k}(x)}{1 - \pi_{\leq t}(x)}.$$

Substituting back into (23) gives

$$\tau_k(x) = \frac{d_{t,k}(x)}{\pi_{t-k}(x)} + \frac{\sum_{j=0}^{t-1} d_{t,j}(x)}{1 - \pi_{\leq t}(x)}, \quad k = 0, 1, \dots, t-1.$$

## C Experimental details

### C.1 Consistency and warm-start experiment

This appendix describes the data-generating process and estimators used in the warm-start experiment in Section 6.2. We use  $T = 5$  time periods and the same staggered-adoption cohort proportions  $\pi = (0.1, 0.2, 0.2, 0.2, 0.2, 0.1)$ , where the last component corresponds to the never-treated group. The covariate is one-dimensional:  $X_i \sim \text{Unif}[-1, 1]$ . The untreated mean is affine in  $X_i$ :

$$\mu_{0,t}(X_i) = \alpha_t + \beta_t X_i, \quad \alpha_t = 0.55 + 0.1(t-1), \quad \beta_t = 0.3 - 0.03(t-1),$$

for  $t = 1, \dots, 5$ . Observed outcomes are generated by

$$Y_{i,t} = \mu_{0,t}(X_i) + \sum_{l=0}^{t-1} \mathbf{1}_{\{A_i=t-l\}} \tau_l(X_i) + \varepsilon_{i,t}, \quad \varepsilon_{i,t} \stackrel{\text{iid}}{\sim} N(0, 0.1^2).$$

For the raw consistency experiments, the lagged CATE vector is

$$(\tau_0(X_i), \dots, \tau_4(X_i)) = (1.3, 1.15, 1.0, 0.85, 0.7 + 0.35X_i).$$

We run these experiments over the sample size

$$N \in \{200, 400, 800, 1600, 3200, 6400, 12800, 25600\}.$$

The trace penalty in the convex relaxation objective is set to  $\lambda_{\text{trace}} = N^{-1/2}$ , while the ridge penalty in the NLS objective is always set to zero.

For the warm-start experiment, the full sample size is fixed at  $N = 25,600$ . We first fit the nonparametric residual-covariance estimator using all covariates and outcomes, but without using the realized assignments. We then reveal the treatment assignments for only a subset  $\mathcal{I}_M \subset \{1, \dots, N\}$  and  $|\mathcal{I}_M| = M$ , where

$$M \in \{25, 50, 100, 200, 400, 800, 1600, 3200\}.$$

We learn the signed CATE vector  $\tau(x)$  using only these  $M$  assignments.

Denote the units that start treatment at time  $a$  or remain untreated at time  $a + l$  by

$$\mathcal{E}_{a,l} = \{i \in \mathcal{I}_M : A_i = a \text{ or } A_i > a + l\},$$

and define the conditional assignment probability

$$e_{a,l} = \frac{\pi_a}{\pi_a + \sum_{b>a+l} \pi_b}.$$

For a candidate lag-CATE function  $f(X_i) = (f_0(X_i), \dots, f_{T-1}(X_i))$ , define

$$\ell_M(f) = \frac{1}{M} \sum_{l=0}^{T-1} \sum_{a=1}^{T-l} \sum_{i \in \mathcal{E}_{a,l}} \left[ \hat{R}_{i,a+l} - \{\mathbf{1}_{\{A_i=a\}} - e_{a,l}\} f_l(X_i) \right]^2,$$

where  $\hat{R}_{i,a+l} = Y_{i,a+l} - \hat{\mu}_{a+l}(X_i)$ , and  $\hat{\mu}_{a+l}(X_i)$  is the fitted outcome function using all covariates and outcomes at time  $a + l$ . The direct R-learner estimator directly learns the lagged CATE from the  $M$  labeled units:

$$\hat{\tau}^{\text{direct}} \in \arg \min_{f \in \mathcal{F}^T} \ell_M(f).$$

The warm-start estimator begins with the assignment-free unsigned estimate  $\hat{\tau}_{\pm}(X_i)$ . Instead of learning the full vector  $f$ , it only learns a sign function  $s(\cdot) \in \{-1, 1\}$  by minimizing the same loss over functions of the form  $f_s(X_i) = s(X_i) \hat{\tau}_{\pm}(X_i)$ . Thus,

$$\hat{s} \in \arg \min_{s \in \mathcal{S}} \ell_M(f_s), \quad \hat{\tau}(\cdot) = \hat{s}(\cdot) \hat{\tau}_{\pm}(\cdot).$$

The warm-start estimator turns the full CATE estimation problem into a lower-dimensional sign-learning problem. Both the direct R-learner and the warm-start sign model are implemented using gradient-boosted regression trees.

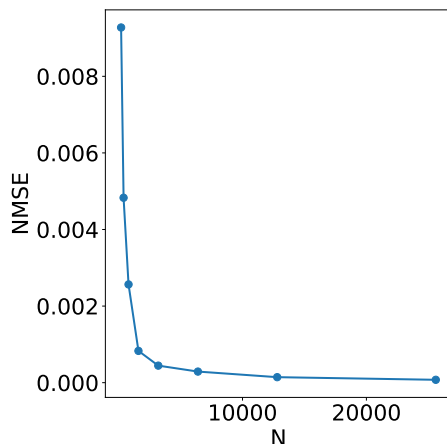


Figure 7: Consistency experiment for the parametric off-diagonal estimator.

## C.2 Parametric estimation

In the main text, we present the off-diagonal estimator in a pointwise, nonparametric form. Here we briefly describe a parametric version. The idea is the same, but we restrict the lagged CATE functions to a finite-dimensional linear model.

Suppose that each lagged CATE is linear in a  $p$ -dimensional feature vector  $\phi(x)$ :

$$\tau_l(x) = \beta_l^\top \phi(x), \quad l = 0, \dots, T-1.$$

Let  $\beta := (\beta_0^\top, \dots, \beta_{T-1}^\top)^\top \in \mathbb{R}^{pT}$ . We write  $\tau(x) = P(x)\beta$ , where  $P(x) := I_T \otimes \phi(x)^\top$ . Substituting this into the off-diagonal quadratic moments gives, for each  $(t, s) \in \mathcal{P}$ ,

$$\tau(x)^\top H_{t,s}(x) \tau(x) = \beta^\top G_{t,s}(x) \beta, \quad G_{t,s}(x) := P(x)^\top H_{t,s}(x) P(x).$$

Thus the same NLS and convex-relaxation estimators from Section 4.3 can be applied after replacing  $H_{t,s}(x)$  by  $G_{t,s}(x)$  and summing the moment-matching loss over the sample. In the convex version, we estimate the rank-one matrix  $\beta\beta^\top$ , extract the leading eigenvector, and obtain a spectral estimator  $\hat{\beta}^{\text{sp}}$ .

We identify the coefficients using the moment conditions

$$\mathbb{E} \left[ \left( R_{i,t} R_{i,s} - \beta^\top G_{t,s}(X_i) \beta \right) \phi_j(X_i) \right] = 0, \quad 1 \leq s < t \leq T, \quad j = 1, \dots, p. \quad (24)$$

These give  $p \binom{T}{2}$  scalar equations for  $pT$  unknown coefficients. For  $T \geq 3$ , the number of equations is at least the number of unknowns. Since the moments are quadratic,  $\beta$  and  $-\beta$  are observationally equivalent. As shown in Proposition 5, a sufficient local identification condition is that the Jacobian of the stacked moment map in (24) with respect to  $\beta$  has full column rank  $pT$  at the true coefficient vector.

We also repeat the consistency experiment under this parametric specification. Figure 7 shows the same pattern as the nonparametric experiment: the estimation error for the coefficient vector  $\beta$  decreases as the sample size grows.

## C.3 County employment experiment

### C.3.1 Data generating process

This appendix describes the semi-synthetic data-generating process used in the county teen employment experiments. We use the standardized log population by  $Z_i$ . We let  $Y^{\text{obs}}$  denote the outcome variable log teen employment, and let  $s_Y := \text{sd}(Y^{\text{obs}})$  be its empirical standard deviation. To generate smooth treatment-effect heterogeneity in the power experiments, we use the centered empirical rank score

$$R_i = \frac{\text{rank}(Z_i) - 1/2}{N}, \quad W_i = 2R_i - 1.$$

We re-randomize treatment timing using the cohort proportions

$$\pi = (0.1, 0.2, 0.2, 0.2, 0.2, 0.1),$$

where the first five components correspond to treatment start times  $1, \dots, 5$ , and the last component corresponds to the never-treated group.

We generate the untreated mean  $\mu_{0,t}(Z_i)$  by perturbing the empirical time- $t$  mean of the original outcome with a nonlinear function of standardized log population:

$$\mu_{0,t}(Z_i) = \bar{Y}_{\cdot,t} + s_Y [a_t Z_i + b_t (Z_i^2 - 1) + c_t (Z_i^3 - 3Z_i)],$$

where  $\bar{Y}_{\cdot,t}$  is the empirical mean of the original outcome at time  $t$ ,

$$\begin{aligned} a &= 2.0 \cdot (-0.9, -0.3, 0.15, 0.75, 1.35), \\ b &= 2.0 \cdot (-0.25, -0.08, 0.08, 0.30, 0.55), \\ c &= 2.0 \cdot (-0.12, -0.03, 0.03, 0.12, 0.28). \end{aligned}$$

In the size experiments, the treatment effect is the sharp zero null:  $\tau_l(Z_i) = 0$ ,  $l = 0, \dots, 4$ . In the power experiment, we let

$$\tau_l(Z_i) = -(m_l + s_l W_i), \quad l = 0, \dots, 4,$$

where  $m = (0.6, 1.0, 1.4, 1.8, 2.2)$  and  $s = (0.4, 0.9, 1.4, 1.9, 2.4)$ . Thus the design has increasingly large negative average effects across exposure lags, with stronger negative effects among higher-log-population counties.

The error covariance is scaled by the variability of the original outcome. Errors have covariance  $(0.3s_Y)^2 I_5$ . Finally, observed outcomes are generated from the additive model in (9) using the re-randomized treatment start times, the untreated mean function above, the corresponding treatment-effect pattern, and the simulated errors.

### C.3.2 Subgroup experiment details

Here we describe the subgroup experiment in the county teen employment study. Denote the raw log population  $X_i = \text{ipop}_i$ . The true threshold is the empirical 0.65-quantile,  $c^* := Q_{0.65}(X_i)$ . The high-lpop group is the effective subgroup,

$$\mathcal{X}_{\text{eff}} = \{i : X_i > c^*\},$$

and the low-lpop group is the true null subgroup,

$$\mathcal{X}_{\text{null}} = \{i : X_i \leq c^*\}.$$

The treated units are approximately evenly assigned to start treatment in periods  $1, \dots, 5$ , with  $A_i = 6$  denoting never treated.

For this subgroup experiment, the untreated potential outcomes are generated as

$$Y_{i,t}(0) = \bar{Y}_{\cdot,t} + \varepsilon_{i,t},$$

where  $\bar{Y}_{\cdot,t}$  is the empirical mean of the original outcome at time  $t$ , and  $\varepsilon_{i,t}$  is standardized Gaussian noise scaled by  $0.04s_Y$ . Unlike the validity and power experiments, this subgroup experiment does not use the nonlinear cubic untreated trend.

For each signal level  $\tau_* \in \{0.10, 0.15, 0.20, 0.25, 0.30\}$ , the treatment effect is invariant over lags and negative in the high-lpop subgroup:

$$\tau_l(X_i) = -\tau_* \mathbf{1}_{\{X_i > c^*\}}, \quad l = 0, \dots, 4.$$

Thus,  $\mathcal{X}_{\text{null}}$  is truly null, while  $\mathcal{X}_{\text{eff}}$  contains affected units.

We estimate the CATE using the diagonal residual-moment estimator described in Section 4.2. The nuisance functions are fitted using CART, with the relevant leaf-size tuning carried out by the out-of-fold threshold-selection procedure. We then apply the assignment-free sign-resolution step from Section 5.1 to obtain signed CATE estimates. Given the fitted signed CATEs  $\hat{\tau}_i$ , we estimate the subgroup threshold by fitting a two-leaf regression stump in  $X_i$ . For a threshold  $c$ , define the left and right groups by

$$\mathcal{L}(c) = \{i : X_i \leq c\}, \quad \mathcal{R}(c) = \{i : X_i > c\}.$$

Let  $\bar{\tau}_L(c)$  and  $\bar{\tau}_R(c)$  denote the average fitted CATEs in the two leaves. The stump loss is

$$\ell(c) = \sum_{i \in \mathcal{L}(c)} \{\hat{\tau}_i - \bar{\tau}_L(c)\}^2 + \sum_{i \in \mathcal{R}(c)} \{\hat{\tau}_i - \bar{\tau}_R(c)\}^2.$$

Since the effective subgroup is assumed to be the high-lpop group with negative treatment effects, we only allow splits satisfying  $\bar{\tau}_R(c) \leq \bar{\tau}_L(c)$ . In each simulation

replication, we draw  $B = 200$  bootstrap resamples. For each bootstrap resample  $b$ , we compute a stump threshold  $\hat{c}^{(b)}$  by minimizing the bootstrap version of  $\ell(c)$ , subject to the direction constraint above and a minimum subgroup-size constraint. The final threshold is the empirical 0.05-quantile of the thresholds:

$$\hat{c} = Q_{0.05}(\hat{c}^{(1)}, \dots, \hat{c}^{(200)}).$$

This lower quantile is used to reduce threshold overshoot. Overshooting the true threshold would place truly affected high-lpop units into the selected null subgroup, which could inflate the rejection rate in the null subgroup.

The selected subgroups used for downstream randomization inference are

$$\hat{\mathcal{X}}_{\text{eff}} = \{i : X_i > \hat{c}\}, \quad \hat{\mathcal{X}}_{\text{null}} = \{i : X_i \leq \hat{c}\}.$$

For subgroup inference, we use the AIPW statistic from Section 5.2. Because the effective subgroup effect is negative, the implementation orients the AIPW statistic using the estimated average signed CATE in the selected subgroup.

## D Technical proofs

### D.1 Proof of Theorem 1

*Proof.* Let  $W := (X_{[N]}, Y_{[N],[T]}, \hat{\eta})$ . Under the sharp null  $H_0$ , the observed outcomes do not depend on the realized assignment vector  $A_{[N]}$ . Conditional on  $W$ , the only randomness in  $T(O_{[N]}; \hat{\eta})$  comes from  $A_{[N]}$ , while the only randomness in  $T(\tilde{O}_{[N]}; \hat{\eta})$  comes from the simulated assignment  $\tilde{A}_{[N]}$ .

The condition  $\hat{\eta} \perp\!\!\!\perp A_{[N]} \mid X_{[N]}, Y_{[N],[T]}$  implies that, conditional on  $W$ , the observed assignment vector still follows the design distribution. By construction,  $\tilde{A}_{[N]}$  is an independent draw from the same design distribution. Hence, conditional on  $W$ , the observed and simulated test statistics  $Z := T(O_{[N]}; \hat{\eta})$  and  $\tilde{Z} := T(\tilde{O}_{[N]}; \hat{\eta})$  have the same distribution. Fix  $W = w$ . Since the assignment space is finite in the randomized designs considered here,  $Z \mid W = w$  has finite support. Let

$$G_w(z) := \tilde{\mathbb{P}}(\tilde{Z} \geq z \mid W = w).$$

The randomization  $p$ -value is  $p(O_{[N]}; \hat{\eta}) = G_W(Z)$ . For any  $\alpha \in (0, 1)$ , define

$$D_\alpha(w) := \{z : G_w(z) \leq \alpha\}.$$

Let  $z_\alpha(w)$  be the smallest support point of  $Z \mid W = w$  that belongs to  $D_\alpha(w)$ . Since  $G_w$  is nonincreasing,  $\{G_w(Z) \leq \alpha\} \subseteq \{Z \geq z_\alpha(w)\}$ . Therefore,

$$\mathbb{P}\{G_w(Z) \leq \alpha \mid W = w\} \leq \mathbb{P}\{Z \geq z_\alpha(w) \mid W = w\} = G_w(z_\alpha(w)) \leq \alpha.$$

Taking conditional expectation given  $(X_{[N]}, Y_{[N],[T]})$  gives

$$\mathbb{P}_{H_0}\{p(O_{[N]}; \hat{\eta}) \leq \alpha \mid X_{[N]}, Y_{[N],[T]}\} \leq \alpha,$$

which proves (5). □

## D.2 Proof of Proposition 1

*Proof.* Fix  $x \in \mathcal{X}$ . Under Assumption 2,  $\tau_l(x) = \tau_*(x)$  for all  $l$ . From (10),

$$R_{i,t} = \tau_*(x) \sum_{l=0}^{t-1} \left( \mathbf{1}_{\{A_i=t-l\}} - \pi_{t-l}(x) \right) + \epsilon_{i,t}.$$

Since

$$\sum_{l=0}^{t-1} \mathbf{1}_{\{A_i=t-l\}} = \mathbf{1}_{\{A_i \leq t\}}, \quad \sum_{l=0}^{t-1} \pi_{t-l}(x) = \pi_{\leq t}(x),$$

we have

$$R_{i,t} = \tau_*(x) \left( \mathbf{1}_{\{A_i \leq t\}} - \pi_{\leq t}(x) \right) + \epsilon_{i,t}.$$

Therefore,

$$\begin{aligned} c_{t,t}(x) &= \mathbb{E}[R_{i,t}^2 \mid X_i = x] \\ &= \tau_*^2(x) \mathbb{E} \left[ \left( \mathbf{1}_{\{A_i \leq t\}} - \pi_{\leq t}(x) \right)^2 \mid X_i = x \right] + \mathbb{E}[\epsilon_{i,t}^2 \mid X_i = x], \end{aligned}$$

where the cross term is zero because  $\mathbb{E}[\epsilon_{i,t} \mid X_i, A_i] = 0$ . Since  $\mathbf{1}_{\{A_i \leq t\}} \mid X_i = x$  is Bernoulli with success probability  $\pi_{\leq t}(x)$ ,

$$\mathbb{E} \left[ \left( \mathbf{1}_{\{A_i \leq t\}} - \pi_{\leq t}(x) \right)^2 \mid X_i = x \right] = \pi_{\leq t}(x)(1 - \pi_{\leq t}(x)).$$

Using  $\mathbb{E}[\epsilon_{i,t}^2 \mid X_i = x] = \sigma_\epsilon^2(x)$ , we obtain

$$c_{t,t}(x) = \tau_*^2(x)v_t(x) + \sigma_\epsilon^2(x), \quad v_t(x) = \pi_{\leq t}(x)(1 - \pi_{\leq t}(x)).$$

□

## D.3 Proof of Proposition 2

*Proof.* By Proposition 1, we have

$$c_{t,t}(x) = \tau_*^2(x)v_t(x) + \sigma_\epsilon^2(x), \quad t \in [T].$$

Averaging over  $t$  gives  $\bar{c}(x) = \tau_*^2(x)\bar{v}(x) + \sigma_\epsilon^2(x)$ . Subtracting yields

$$c_{t,t}(x) - \bar{c}(x) = \tau_*^2(x)\{v_t(x) - \bar{v}(x)\}.$$

If  $v_t(x) \neq \bar{v}(x)$ , then

$$\tau_*^2(x) = \frac{c_{t,t}(x) - \bar{c}(x)}{v_t(x) - \bar{v}(x)}.$$

Thus  $m_*(x) = |\tau_*(x)|$  is identified by taking the nonnegative square root.  $\square$

## D.4 Proof of Proposition 3

*Proof.* Since  $T$  is fixed and  $\hat{c}_{t,t}(x) \xrightarrow{p} c_{t,t}(x)$  for all  $t$ ,

$$\hat{\bar{c}}(x) = \frac{1}{T} \sum_{t=1}^T \hat{c}_{t,t}(x) \xrightarrow{p} \bar{c}(x).$$

Hence

$$\frac{\hat{c}_{t,t}(x) - \hat{\bar{c}}(x)}{v_t(x) - \bar{v}(x)} \xrightarrow{p} \frac{c_{t,t}(x) - \bar{c}(x)}{v_t(x) - \bar{v}(x)} = \tau_*^2(x),$$

where the last equality follows from Proposition 2. Since the map  $u \mapsto \sqrt{\max\{u, 0\}}$  is continuous,

$$\hat{m}_*(x) = \sqrt{\max\left\{\frac{\hat{c}_{t,t}(x) - \hat{\bar{c}}(x)}{v_t(x) - \bar{v}(x)}, 0\right\}} \xrightarrow{p} \sqrt{\tau_*^2(x)} = m_*(x).$$

$\square$

## D.5 Proof of Proposition 4

*Proof.* Fix  $x \in \mathcal{X}$  and  $1 \leq s < t \leq T$ . Throughout, condition on  $X_i = x$ . Let

$$\Delta_a := \mathbf{1}_{\{A_i=a\}} - \pi_a(x), \quad a \in [T].$$

Then (10) gives

$$R_{i,t} = \sum_{l=0}^{t-1} \Delta_{t-l} \tau_l(x) + \epsilon_{i,t}, \quad R_{i,s} = \sum_{k=0}^{s-1} \Delta_{s-k} \tau_k(x) + \epsilon_{i,s}.$$

Under Assumption 4,  $\mathbb{E}[\epsilon_{i,t} \epsilon_{i,s} \mid X_i = x] = 0$  for  $t \neq s$ . The cross terms involving one  $\epsilon$  are also zero by  $\mathbb{E}[\epsilon_{i,t} \mid X_i, A_i] = 0$ . Therefore,

$$c_{t,s}(x) = \sum_{l=0}^{t-1} \sum_{k=0}^{s-1} \mathbb{E}[\Delta_{t-l} \Delta_{s-k} \mid X_i = x] \tau_l(x) \tau_k(x).$$

For  $a, b \in [T]$ , mutual exclusivity of the treatment start indicators gives

$$\mathbb{E}[\Delta_a \Delta_b \mid X_i = x] = \pi_a(x) \mathbf{1}_{\{a=b\}} - \pi_a(x) \pi_b(x).$$

Substituting  $a = t - l$  and  $b = s - k$ , and using  $t > s$ , we obtain

$$c_{t,s}(x) = \sum_{k=0}^{s-1} \pi_{s-k}(x) \tau_{t-s+k}(x) \tau_k(x) - \bar{\tau}_t(x) \bar{\tau}_s(x), \quad (25)$$

where  $\bar{\tau}_t(x) := \sum_{l=0}^{t-1} \pi_{t-l}(x) \tau_l(x)$ . To write the moment as a quadratic form, define

$$\pi^{(t)}(x) := (\pi_t(x), \pi_{t-1}(x), \dots, \pi_1(x), 0, \dots, 0)^\top \in \mathbb{R}^T,$$

$$\pi^{(s)}(x) := (\pi_s(x), \pi_{s-1}(x), \dots, \pi_1(x), 0, \dots, 0)^\top \in \mathbb{R}^T,$$

$$D_s(x) := \text{diag}(\pi_s(x), \pi_{s-1}(x), \dots, \pi_1(x), 0, \dots, 0) \in \mathbb{R}^{T \times T},$$

and let  $J_{t-s} \in \mathbb{R}^{T \times T}$  be the shift matrix with entries

$$(J_{t-s})_{a,b} = \mathbf{1}_{\{a=b+t-s\}}.$$

Then

$$\tau(x)^\top J_{t-s} D_s(x) \tau(x) = \sum_{k=0}^{s-1} \pi_{s-k}(x) \tau_{t-s+k}(x) \tau_k(x),$$

and

$$\tau(x)^\top \pi^{(t)}(x) \pi^{(s)}(x)^\top \tau(x) = \bar{\tau}_t(x) \bar{\tau}_s(x).$$

Thus, with

$$G_{t,s}(x) := J_{t-s} D_s(x) - \pi^{(t)}(x) \pi^{(s)}(x)^\top,$$

we have  $c_{t,s}(x) = \tau(x)^\top G_{t,s}(x) \tau(x)$ . Since only the symmetric part matters in a scalar quadratic form, define

$$H_{t,s}(x) := \frac{1}{2} \{G_{t,s}(x) + G_{t,s}(x)^\top\}.$$

Then  $c_{t,s}(x) = \tau(x)^\top H_{t,s}(x) \tau(x)$ , which proves the quadratic representation.  $\square$

## D.6 Proof of Proposition 5

*Proof.* Fix  $x \in \mathcal{X}$ , and write  $F := F_x$ ,  $J := J_x$ , and  $\tau_0 := \tau(x)$ . By assumption,  $\tau_0 \neq 0$  and  $J(\tau_0)$  has full column rank  $T$ . Hence there is a set of  $T$  coordinates  $\mathcal{I} \subseteq \mathcal{P}$  such that the submatrix  $J_{\mathcal{I}}(\tau_0)$  is invertible. Let  $P_{\mathcal{I}}$  be the coordinate projection onto these entries, and define

$$G := P_{\mathcal{I}} \circ F : \mathbb{R}^T \rightarrow \mathbb{R}^T.$$

Then  $DG(\tau_0) = J_{\mathcal{I}}(\tau_0)$  is invertible. By the inverse function theorem, there exists an open neighborhood  $U_+$  of  $\tau_0$  on which  $G$ , and therefore  $F$ , is injective.

Because each component of  $F$  is a quadratic form,  $F(-\tau) = F(\tau)$  for every  $\tau$ . Also,  $J(-\tau_0) = -J(\tau_0)$ , so  $J(-\tau_0)$  has full column rank. Applying the same argument at  $-\tau_0$ , there is an open neighborhood  $U_-$  of  $-\tau_0$  on which  $F$  is injective.

Choose an open neighborhood  $\mathcal{N}_x$  of  $\tau_0$  small enough that  $\mathcal{N}_x \subseteq U_+$ ,  $-\mathcal{N}_x \subseteq U_-$ , and  $\mathcal{N}_x \cap (-\mathcal{N}_x) = \emptyset$ . Since the population moment restriction is  $c(x) = F(\tau_0)$ , injectivity on  $\mathcal{N}_x$  gives

$$\{\tau \in \mathcal{N}_x : F(\tau) = c(x)\} = \{\tau_0\}.$$

If  $\tau \in -\mathcal{N}_x$  and  $F(\tau) = c(x)$ , then  $-\tau \in \mathcal{N}_x$  and, by evenness of  $F$ ,

$$F(-\tau) = F(\tau) = F(\tau_0).$$

Injectivity on  $\mathcal{N}_x$  gives  $-\tau = \tau_0$ , or  $\tau = -\tau_0$ . Therefore,

$$\{\tau \in \mathcal{N}_x \cup (-\mathcal{N}_x) : F_x(\tau) = c(x)\} = \{\tau(x), -\tau(x)\}.$$

□

## D.7 Proof of Proposition 6

*Proof.* Recall that the rows of  $J_x(\tau(x))$  are proportional to

$$\{H_{t,s}(x)\tau(x) : (t, s) \in \mathcal{P}\}.$$

Thus it suffices to find  $T$  pairs  $(t, s) \in \mathcal{P}$  such that the corresponding vectors  $H_{t,s}(x)\tau(x)$  span  $\mathbb{R}^T$ .

Let  $e_0, \dots, e_{T-1}$  denote the standard basis of  $\mathbb{R}^T$ . Recall from the quadratic-form representation that

$$H_{t,s}(x) = \frac{1}{2}\{G_{t,s}(x) + G_{t,s}(x)^\top\},$$

where

$$G_{t,s}(x) = J_{t-s}D_s(x) - \pi^{(t)}(x)\pi^{(s)}(x)^\top.$$

Here

$$D_s(x) = \text{diag}(\pi_s(x), \pi_{s-1}(x), \dots, \pi_1(x), 0, \dots, 0),$$

$$\pi^{(t)}(x) = (\pi_t(x), \pi_{t-1}(x), \dots, \pi_1(x), 0, \dots, 0)^\top,$$

and  $J_{t-s}$  is the shift matrix with entries

$$(J_{t-s})_{a,b} = \mathbf{1}_{\{a=b+t-s\}}, \quad a, b \in \{0, \dots, T-1\},$$

where indices follow the lag coordinates of  $\tau(x) = (\tau_0(x), \dots, \tau_{T-1}(x))^\top$ .

Under the equal-probability design  $\pi_1(x) = \dots = \pi_T(x) = q$ , we have

$$D_s(x) = qD_s^0, \quad \pi^{(t)}(x) = q\pi_0^{(t)}, \quad \pi^{(s)}(x) = q\pi_0^{(s)},$$

where

$$D_s^0 = \text{diag}(\underbrace{1, \dots, 1}_s, 0, \dots, 0).$$

Therefore,

$$\begin{aligned} G_{t,s}(x) &= J_{t-s}D_s(x) - \pi^{(t)}(x)\pi^{(s)}(x)^\top \\ &= qJ_{t-s}D_s^0 - q^2\pi_0^{(t)}\{\pi_0^{(s)}\}^\top. \end{aligned}$$

Taking the symmetric part gives

$$H_{t,s}(x) = \frac{q}{2} \{J_{t-s}D_s^0 + D_s^0J_{t-s}^\top\} - \frac{q^2}{2} \left\{ \pi_0^{(t)}\{\pi_0^{(s)}\}^\top + \pi_0^{(s)}\{\pi_0^{(t)}\}^\top \right\}.$$

In particular,

$$H_{t,s}(x) = \frac{q}{2} \{J_{t-s}D_s^0 + D_s^0J_{t-s}^\top\} + O(q^2).$$

Now consider the  $T$  off-diagonal pairs

$$(2, 1), (3, 1), \dots, (T, 1), \quad (3, 2).$$

These give  $T - 1$  pairs involving the first time point, plus one additional pair (3, 2), yielding  $T$  candidate rows of the Jacobian.

For  $j = 1, \dots, T - 1$ , the leading-order vector from the pair  $(j + 1, 1)$  is proportional to

$$v_j := \tau_j(x)e_0 + \tau_0(x)e_j.$$

The leading-order vector from the pair (3, 2) is proportional to

$$v_* := \tau_1(x)e_0 + \{\tau_0(x) + \tau_2(x)\}e_1 + \tau_1(x)e_2.$$

Let  $V(\tau(x))$  be the  $T \times T$  matrix with rows

$$v_1^\top, \dots, v_{T-1}^\top, v_*^\top.$$

A direct determinant calculation gives

$$\det\{V(\tau(x))\} = (-1)^T 2 \tau_0(x)^{T-2} \tau_1(x) \tau_2(x),$$

up to the sign convention from row ordering.

Under the geometric decay model,

$$\tau_l(x) = \theta(x)\rho^l, \quad l = 0, \dots, T-1,$$

we have

$$\tau_0(x) = \theta(x), \quad \tau_1(x) = \theta(x)\rho, \quad \tau_2(x) = \theta(x)\rho^2.$$

Therefore,

$$\det\{V(\tau(x))\} = (-1)^T 2\theta(x)^T \rho^3,$$

which is nonzero whenever  $\theta(x) \neq 0$  and  $\rho \in (0, 1)$ .

For finite  $q$ , let  $V_q(\tau(x))$  be the  $T \times T$  matrix formed by the selected vectors  $H_{t,s}(x)\tau(x)$ . Since each entry of  $H_{t,s}(x)\tau(x)$  is a polynomial in  $q$ ,  $\det\{V_q(\tau(x))\}$  is also a polynomial in  $q$ . Moreover, from the expansion above,

$$V_q(\tau(x)) = \frac{q}{2}V(\tau(x)) + O(q^2),$$

and hence

$$\det\{V_q(\tau(x))\} = \left(\frac{q}{2}\right)^T \det\{V(\tau(x))\} + O(q^{T+1}).$$

Substituting the geometric-decay form gives

$$\det\{V_q(\tau(x))\} = \theta(x)^T [(-1)^T 2^{1-T} \rho^3 q^T + O(q^{T+1})].$$

Define

$$P_{T,\rho}(q) := \theta(x)^{-T} \det\{V_q(\tau(x))\}.$$

Then  $P_{T,\rho}(q)$  is a polynomial in  $q$ , and its leading term is

$$(-1)^T 2^{1-T} \rho^3 q^T,$$

which is not identically zero because  $\rho \in (0, 1)$ . Hence  $P_{T,\rho}$  is a nonzero polynomial.

Whenever  $P_{T,\rho}(q) \neq 0$ , we have

$$\det\{V_q(\tau(x))\} \neq 0.$$

Thus the selected vectors  $H_{t,s}(x)\tau(x)$  span  $\mathbb{R}^T$ , and therefore the full collection

$$\{H_{t,s}(x)\tau(x) : (t, s) \in \mathcal{P}\}$$

also spans  $\mathbb{R}^T$ . Consequently,

$$\text{rank}(J_x(\tau(x))) = T.$$

□

## D.8 Proof of Proposition 7

*Proof.* Fix  $x \in \mathcal{X}$ , and write  $\tau_0 := \tau(x)$ . Since the population moment equation holds,

$$c(x) = F_x(\tau_0).$$

Also, because  $F_x$  is quadratic,  $F_x(-\tau_0) = F_x(\tau_0) = c(x)$ . Hence

$$\{\tau_0, -\tau_0\} \subseteq \{\tau \in \Theta : F_x(\tau) = c(x)\}.$$

It remains to show the reverse inclusion. Suppose, toward a contradiction, that there exists  $\tau' \in \Theta$  such that  $F_x(\tau') = c(x)$ ,  $\tau' \notin \{\tau_0, -\tau_0\}$ . Then

$$d_{\pm}(\tau', \tau_0) = \min\{\|\tau' - \tau_0\|_2, \|\tau' + \tau_0\|_2\} > 0.$$

Let  $\varepsilon = d_{\pm}(\tau', \tau_0)/2$ . Then  $\tau'$  belongs to the set

$$\{\tau \in \Theta : d_{\pm}(\tau, \tau_0) \geq \varepsilon\}.$$

By the assumed separation condition,

$$\|F_x(\tau') - c(x)\|_2^2 \geq \inf_{\tau \in \Theta: d_{\pm}(\tau, \tau_0) \geq \varepsilon} \|F_x(\tau) - c(x)\|_2^2 > 0.$$

This contradicts  $F_x(\tau') = c(x)$ . Therefore no such  $\tau'$  exists, and

$$\{\tau \in \Theta : F_x(\tau) = c(x)\} = \{\tau_0, -\tau_0\}.$$

Finally, since  $\tau_0 \tau_0^\top = (-\tau_0)(-\tau_0)^\top$ , the rank-one matrix

$$B(x) := \tau(x)\tau(x)^\top$$

is uniquely determined by the moment equation over  $\Theta$ . This proves the claim.  $\square$

## D.9 Proof of Proposition 8

*Proof.* Fix a unit  $i$ , and condition on  $X_i$  and  $A_i = a \leq T$ . Define

$$g_{i,t} := \sum_{l=0}^{t-1} \left( \mathbf{1}_{\{a=t-l\}} - \pi_{t-l}(X_i) \right) \theta(X_i) \rho^l, \quad t \in [T].$$

Under the assumed CATE form

$$\tau_l(X_i) = s_i \theta(X_i) \rho^l,$$

the residual equation in (10) becomes

$$R_{i,t} = s_i g_{i,t} + \epsilon_{i,t}, \quad t \in [T].$$

The oracle sign estimator with observed assignment compares the two losses

$$L_i(s) := \sum_{t=1}^T (R_{i,t} - s g_{i,t})^2, \quad s \in \{-1, 1\}.$$

For the correct sign,

$$L_i(s_i) = \sum_{t=1}^T \epsilon_{i,t}^2.$$

For the wrong sign,

$$L_i(-s_i) = \sum_{t=1}^T (\epsilon_{i,t} + 2s_i g_{i,t})^2.$$

Thus,

$$\{\hat{s}_i^{\text{obs}} \neq s_i\} \subseteq \{L_i(-s_i) \leq L_i(s_i)\}.$$

Expanding  $L_i(-s_i) \leq L_i(s_i)$  gives

$$4 \sum_{t=1}^T g_{i,t}^2 + 4s_i \sum_{t=1}^T \epsilon_{i,t} g_{i,t} \leq 0,$$

or equivalently,

$$s_i \sum_{t=1}^T \epsilon_{i,t} g_{i,t} \leq - \sum_{t=1}^T g_{i,t}^2.$$

By the conditional sub-Gaussian assumption,

$$s_i \sum_{t=1}^T \epsilon_{i,t} g_{i,t}$$

is sub-Gaussian with variance proxy

$$\sigma^2 \sum_{t=1}^T g_{i,t}^2.$$

Therefore, by the sub-Gaussian tail bound,

$$\mathbb{P}(\hat{s}_i^{\text{obs}} \neq s_i \mid X_i, A_i = a) \leq \exp \left\{ -\frac{1}{2\sigma^2} \sum_{t=1}^T g_{i,t}^2 \right\}.$$

It remains to lower bound  $\sum_{t=1}^T g_{i,t}^2$ . Under the balanced assignment design,

$$\pi_1(X_i) = \cdots = \pi_T(X_i) = \frac{1}{T+1}.$$

At the adoption time  $t = a$ ,

$$g_{i,a} = \theta(X_i) \left[ 1 - \frac{1}{T+1} \sum_{l=0}^{a-1} \rho^l \right] = \theta(X_i) \left[ 1 - \frac{1}{T+1} \frac{1-\rho^a}{1-\rho} \right].$$

Since  $\sum_{t=1}^T g_{i,t}^2 \geq g_{i,a}^2$ , we have

$$\sum_{t=1}^T g_{i,t}^2 \geq \theta^2(X_i) \left[ 1 - \frac{1}{T+1} \frac{1-\rho^a}{1-\rho} \right]^2.$$

Also,

$$\frac{1-\rho^a}{1-\rho} = 1 + \rho + \cdots + \rho^{a-1} \leq a,$$

because  $\rho \in (0, 1)$ . Hence

$$1 - \frac{1}{T+1} \frac{1-\rho^a}{1-\rho} \geq 1 - \frac{a}{T+1} > 0.$$

Thus,

$$\sum_{t=1}^T g_{i,t}^2 \geq \theta^2(X_i) \left( 1 - \frac{a}{T+1} \right)^2.$$

Substituting this lower bound into the tail inequality gives

$$\mathbb{P}(\hat{s}_i^{\text{obs}} \neq s_i \mid X_i, A_i = a) \leq \exp \left\{ -\frac{\theta^2(X_i)}{2\sigma^2} \left( 1 - \frac{a}{T+1} \right)^2 \right\}.$$

This proves the claim. □

## D.10 Proof of Theorem 2

*Proof.* Fix  $x \in \mathcal{X}_0$ , and write

$$c_0 := c(x), \quad \hat{c} := \hat{c}(x), \quad B_0 := B(x) = \tau(x)\tau(x)^\top.$$

Let

$$J_x^0(B) := \ell^{\text{cvx}}(B; c, x, 0), \quad \hat{J}_x(B) := \ell^{\text{cvx}}(B; \hat{c}, x, \lambda_N),$$

where  $\lambda_N = o(1)$ . The minimization is over

$$\mathbb{B} = \{B \succeq 0 : \text{tr}(B) \leq M^2\}.$$

Set  $r_N := \|\hat{c} - c_0\|_2$ , so  $r_N \xrightarrow{p} 0$  by Assumption 5.

By Assumption 6,

$$C_H := \max_{(t,s) \in \mathcal{P}} \|H_{t,s}(x)\|_{\text{op}} < \infty.$$

For any  $B \in \mathbb{B}$ ,

$$|\text{tr}(H_{t,s}(x)B)| \leq \|H_{t,s}(x)\|_{\text{op}} \text{tr}(B) \leq C_H M^2.$$

Thus  $\sup_{B \in \mathbb{B}} \|\mathcal{A}_x(B)\|_2 < \infty$ . For any  $B \in \mathbb{B}$ ,

$$\begin{aligned} \hat{J}_x(B) - J_x^0(B) &= \|\hat{c} - \mathcal{A}_x(B)\|_2^2 - \|c_0 - \mathcal{A}_x(B)\|_2^2 + \lambda_N \text{tr}(B) \\ &= 2(c_0 - \mathcal{A}_x(B))^\top (\hat{c} - c_0) + \|\hat{c} - c_0\|_2^2 + \lambda_N \text{tr}(B). \end{aligned}$$

Therefore,

$$\sup_{B \in \mathbb{B}} |\hat{J}_x(B) - J_x^0(B)| \leq 2r_N \sup_{B \in \mathbb{B}} \|c_0 - \mathcal{A}_x(B)\|_2 + r_N^2 + \lambda_N M^2 \xrightarrow{p} 0.$$

Fix  $\varepsilon > 0$ , and define

$$\mathbb{B}_\varepsilon := \{B \in \mathbb{B} : \|B - B_0\|_F \geq \varepsilon\}.$$

Since  $\mathbb{B}$  is compact and  $J_x^0$  is continuous,  $\mathbb{B}_\varepsilon$  is compact. Since  $B_0$  is the unique minimizer of  $J_x^0$ ,

$$\delta_\varepsilon := \inf_{B \in \mathbb{B}_\varepsilon} J_x^0(B) - J_x^0(B_0) > 0.$$

On the event

$$\sup_{B \in \mathbb{B}} |\hat{J}_x(B) - J_x^0(B)| \leq \delta_\varepsilon/3,$$

which has probability tending to one, every  $B \in \mathbb{B}_\varepsilon$  has strictly larger sample objective than  $B_0$ . Hence no minimizer  $\hat{B}(x)$  can lie in  $\mathbb{B}_\varepsilon$ . This proves

$$\|\hat{B}(x) - B_0\|_F \xrightarrow{p} 0.$$

For the spectral part, let  $\tau_0 := \tau(x)$ ,  $u_0 := \tau_0 / \|\tau_0\|_2$ , and  $g_0 := \|\tau_0\|_2^2$ . Then  $B_0 = g_0 u_0 u_0^\top$ , with eigengap  $g_0 \geq c_\tau^2 > 0$ . Since  $\|\hat{B}(x) - B_0\|_{\text{op}} \leq \|\hat{B}(x) - B_0\|_F \rightarrow 0$  in probability, Weyl's inequality gives  $\hat{\lambda}_1(x) \xrightarrow{p} g_0$ . Moreover,  $B_0$  has eigengap  $g_0 = \|\tau(x)\|_2^2 \geq c_\tau^2 > 0$ , so Davis–Kahan gives

$$\min\{\|\hat{u}_1(x) - u_0\|_2, \|\hat{u}_1(x) + u_0\|_2\} \xrightarrow{p} 0.$$

Combining the eigenvalue convergence with the eigenvector convergence up to sign yields

$$d_\pm \left( \sqrt{\hat{\lambda}_1(x)} \hat{u}_1(x), \tau(x) \right) = d_\pm(\hat{\tau}_\pm^{\text{SP}}(x), \tau(x)) \xrightarrow{p} 0.$$

This proves consistency up to a global sign.  $\square$

## D.11 Proof of Theorem 3

*Proof.* Fix  $x \in \mathcal{X}_0$ , and write

$$c_0 := c(x), \quad \hat{c} := \hat{c}(x), \quad \tau_0 := \tau(x).$$

Let

$$L_x^0(\tau) := \ell^{\text{nls}}(\tau; c, x, 0), \quad \hat{L}_x(\tau) := \ell^{\text{nls}}(\tau; \hat{c}, x, \rho_N),$$

where  $\rho_N = o(1)$ . The minimization is over  $\Theta = \{\tau \in \mathbb{R}^T : \|\tau\|_2 \leq M\}$ . Set  $r_N := \|\hat{c} - c_0\|_2$ , so  $r_N \xrightarrow{p} 0$ .

By Assumption 6,  $C_H := \max_{(t,s) \in \mathcal{P}} \|H_{t,s}(x)\|_{\text{op}} < \infty$ . For any  $\tau \in \Theta$ ,

$$|(F_x(\tau))_{t,s}| = |\tau^\top H_{t,s}(x) \tau| \leq C_H M^2,$$

so  $\sup_{\tau \in \Theta} \|F_x(\tau)\|_2 < \infty$ . For any  $\tau \in \Theta$ ,

$$\begin{aligned} \hat{L}_x(\tau) - L_x^0(\tau) &= \|\hat{c} - F_x(\tau)\|_2^2 - \|c_0 - F_x(\tau)\|_2^2 + \rho_N \|\tau\|_2^2 \\ &= 2(c_0 - F_x(\tau))^\top (\hat{c} - c_0) + \|\hat{c} - c_0\|_2^2 + \rho_N \|\tau\|_2^2. \end{aligned}$$

Thus,

$$\sup_{\tau \in \Theta} |\hat{L}_x(\tau) - L_x^0(\tau)| \leq 2r_N \sup_{\tau \in \Theta} \|c_0 - F_x(\tau)\|_2 + r_N^2 + \rho_N M^2 \xrightarrow{p} 0.$$

Fix  $\varepsilon > 0$ , and define

$$\Theta_\varepsilon := \{\tau \in \Theta : \min\{\|\tau - \tau_0\|_2, \|\tau + \tau_0\|_2\} \geq \varepsilon\}.$$

Since  $\Theta$  is compact and  $L_x^0$  is continuous,  $\Theta_\varepsilon$  is compact. By assumption, the unique minimizer set of  $L_x^0$  is  $\{\tau_0, -\tau_0\}$ . Hence

$$\eta_\varepsilon := \inf_{\tau \in \Theta_\varepsilon} L_x^0(\tau) - L_x^0(\tau_0) > 0.$$

On the event  $\sup_{\tau \in \Theta} |\hat{L}_x(\tau) - L_x^0(\tau)| \leq \eta_\varepsilon/3$ , which has probability tending to one, every  $\tau \in \Theta_\varepsilon$  has strictly larger sample objective than  $\tau_0$ . Therefore no global minimizer  $\hat{\tau}^{\text{nls}}(x)$  lies in  $\Theta_\varepsilon$ . Since  $\varepsilon > 0$  is arbitrary,

$$d_\pm(\hat{\tau}_\pm^{\text{nls}}(x), \tau(x)) \xrightarrow{p} 0.$$

□